

Backfolding of RecA-coated DNA confined beyond the Odijk regime

Toby St Clere Smithe

May 21, 2015

Abstract

An analysis of data from microchannel-confinement experiments on RecA-coated DNA shows less backfolding than simulations of the wormlike chain (WLC) model in the transition out of the Odijk regime. A comparison of experimental results with simulations of the WLC model is presented.

Contents

1	Introduction and methodology	3
1.1	Extension computation	3
1.2	Contour length computation	3
1.3	Rejection criteria	3
2	Results and discussion	4
2.1	Conclusions and further questions	7
2.2	Plots for each channel separately; both DNA types	8
2.3	Plots for T4 DNA only	14
2.4	Plots for λ DNA only	20
2.5	Rejected configurations	25
3	Classification of conformations and experimental conditions	27
3.1	Summary	27
3.2	Tables	29
4	Kymographs	37
4.1	130603-RecA-T4-wide-2	37
4.2	130603-RecA-T4-wide-3	38
4.3	130603-RecA-T4-wide-4	38
4.4	130603-RecA-T4-wide-5	39
4.5	130603-RecA-T4-wide-7	40
4.6	130607-RecA-T4-narrow-10	41
4.7	130607-RecA-T4-narrow-7	42
4.8	130607-RecA-T4-narrow-8	43
4.9	130607-RecA-T4-narrow-9	44
4.10	130607-RecA-T4-wide-1	45
4.11	130607-RecA-T4-wide-2	46
4.12	130607-RecA-T4-wide-3	47
4.13	130607-RecA-T4-wide-4	48
4.14	130607-RecA-T4-wide-5	49
4.15	130607-RecA-T4-wide-6	50
4.16	130905-RecA-T4-narrow-1	51

4.17	130905-RecA-T4-narrow-2	52
4.18	130905-RecA-T4-narrow-3	53
4.19	130905-RecA-T4-narrow-4	53
4.20	130905-RecA-T4-narrow-5	54
4.21	130905-RecA-T4-narrow-6	54
4.22	130905-RecA-T4-narrow-7	55
4.23	130905-RecA-T4-wide-1	56
4.24	130905-RecA-T4-wide-2	57
4.25	130905-RecA-T4-wide-3	58
4.26	130905-RecA-T4-wide-4	59
4.27	130905-RecA-T4-wide-5	60
4.28	130905-RecA-T4-wide-6	61
4.29	130905-RecA-T4-wide-7	62
4.30	130905-RecA-T4-wide-8	63
4.31	130924-RecA-lambda-narrow-1	64
4.32	130924-RecA-lambda-narrow-2	65
4.33	130924-RecA-lambda-narrow-3	66
4.34	130924-RecA-lambda-narrow-4	67
4.35	130924-RecA-lambda-narrow-5	68
4.36	130924-RecA-lambda-narrow-6	69
4.37	130924-RecA-lambda-wide-1	70
4.38	130924-RecA-lambda-wide-10	71
4.39	130924-RecA-lambda-wide-2	72
4.40	130924-RecA-lambda-wide-3	73
4.41	130924-RecA-lambda-wide-4	74
4.42	130924-RecA-lambda-wide-5	75
4.43	130924-RecA-lambda-wide-8	76
4.44	130924-RecA-lambda-wide-9	77

1 Introduction and methodology

In the experiments presented here, channels were used with a height of 140 nm – thereby constraining the filaments not to fluctuate in this dimension – and widths of 600 nm to 3000 nm. Filaments are funneled from a channel of one width to a channel of another width, in increasing or decreasing order. In this way, it is possible to study the changing conformation of the filament as the channel width changes. Both T4 and λ DNA were used, with the contour lengths of the coated T4 DNA ranging from 7 microns to 21 microns, and the λ DNA ranging from 11 microns to 23 microns; the different DNA types do not produce qualitatively different results under the analysis presented here.

Dorfman et al have made simulations of the worm-like chain model in the regime of interest, using channel dimensions similar to those employed experimentally. Here, these simulations are compared with the experimental results. Data describing the contour lengths L and linear extensions X were extracted from microscopy videos produced by Frykholm. The persistence length of RecA-coated dsDNA was taken to be 1.15 m, as reported by Frykholm et al [1], and in agreement with other estimates [2].

Plots of $\langle X \rangle / L$ against L/l_p were produced, in order to compare with the simulated results; simulated values were inferred by inspection of the plot by Dorfman. The amount of fluctuation of the filament is quantified by the ratio $\langle X \rangle / L$: where this value is near 1, the filament is mostly straight, and smaller values indicate progressively larger fluctuations or backfolding.

1.1 Extension computation

Each video of a single channel width contains 300 or 400 frames, sampled at approximately one frame every 0.11 seconds, and there can be up to six videos – one for each width – for a single filament in a single experiment. To estimate the extensions, X , of the molecule represented in these frames, the frames were first passed through a median filter with a radius of 2, and then the maximum pixel intensity in each column was taken to provide an intensity profile along the channel. Next, a moving average (in time) of window size 3 frames and then (in space) of window size 4 pixels was computed using these intensity profiles. Finally, an error function ‘box’ curve was least-squares fitted to each such average. This was then averaged along the channel to compute the extension.

1.2 Contour length computation

For each molecule, a random subset of frames from the corresponding microscopy videos was presented on screen. Frames were selected from the recordings of the molecule in all the channels for which data were available. The contour lengths were then computed by tracing a path over the molecule filament on each frame using the computer mouse and then calculating the length of this path, until an adequate number of paths (at least 40) was sampled. The mean and standard deviation of these paths were then computed for each molecule in the data set.

1.3 Rejection criteria

There were two rejection criteria for the data. Firstly, if the kymographs suggested experimental error (such as a ‘tangled’ molecule or a molecule becoming folded during the transition between channels of different widths), which was then supported by inspection of the microscope images; see below for examples. Secondly, data were rejected if the standard deviations of either $\langle X \rangle / L$ or L exceeded 40% of the computed values; this occurred for a total of 10 data points across 6 experiments.

2 Results and discussion

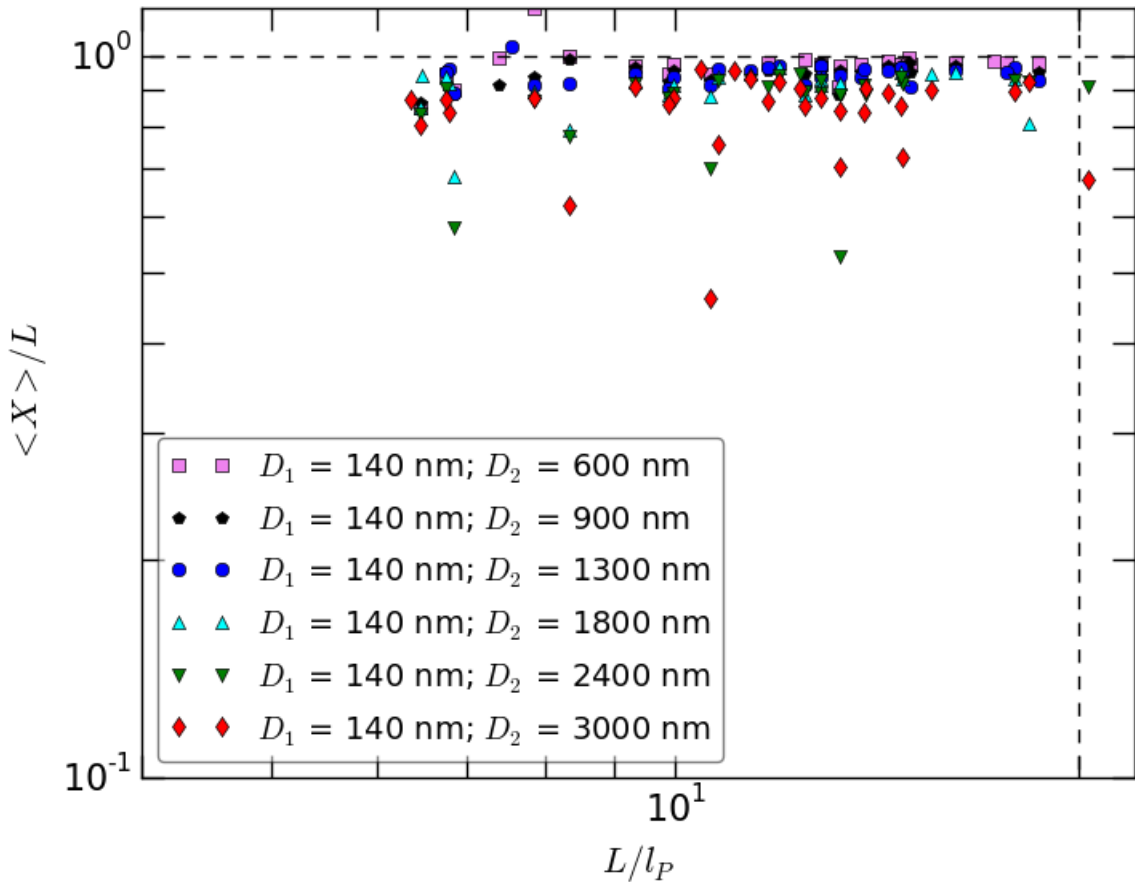


Figure 1: Experimental data for both T4 and λ DNA on log axes. The dashed vertical line is the dashed line in 2.

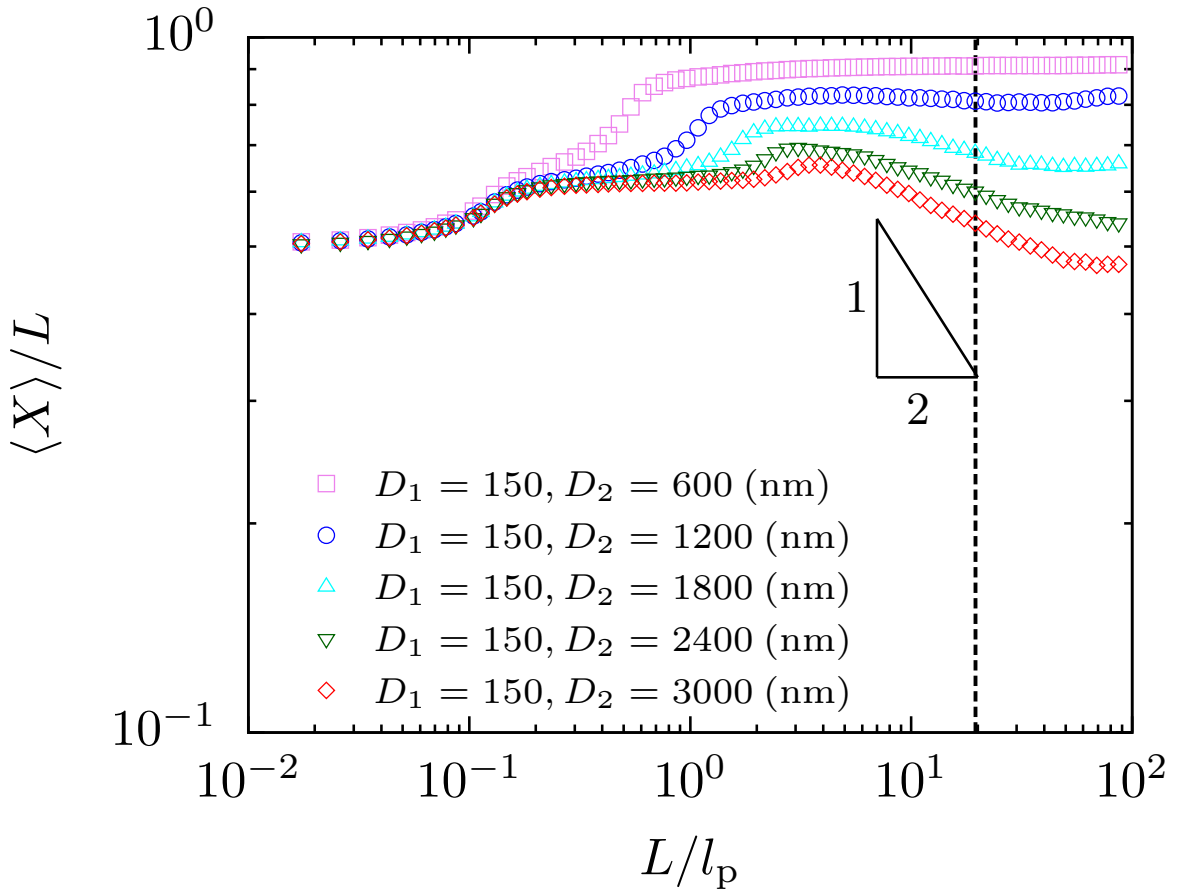


Figure 2: Simulated data, from Dorfman (without rescaling).

Having excluded the experimentally suspicious cases, of 65697 remaining frames, 61345 were accepted according to the criteria described above (93.4%). Some examples of accepted and rejected configurations are given at the end of this report. For the different channel widths, the acceptance rates are: 98.9% (600nm), 99.9% (900nm), 96.1% (1300nm), 91.6% (1800nm), 86.0% (2400nm), and 90.3% (3000nm). More details about the rejected configurations are given below.

Some results show $\langle X \rangle > L$, and so it is important to note that the quantity by which $\langle X \rangle / L - 1$ is less than one standard deviation of $\langle X \rangle / L$.

The accepted data for both DNA types are plotted in Figure 1, which has axes to match the simulated data, plotted in Figure 2. Figures 8 to 13 show the data and simulations plotted on log axes separately for each channel width. Moreover, Figures 14 to 25 show the data and simulations, on linear axes for clarity, for the T4 and λ DNA separately, showing no significant difference.

A slight increase in the size of the fluctuations is visible given increasing channel width, but not of the same magnitude as predicted by simulations. Moreover, the negative slope for the larger channel sizes seen in Figure 2 is not visible in the experimental data: this slope represents the increased possibility of backfolding given a length of numerous multiples of the persistence length, and sufficient space in which to make those turns.

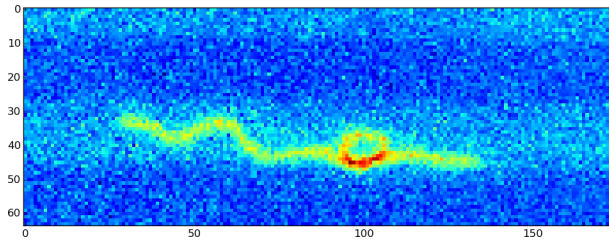


Figure 3: 130924-RecA-lambda-wide-2 ($L/l_P = 20.30$) at frame 131 in the 3000nm channel

There are nonetheless, evident in the wider channels, three molecules whose $\langle X \rangle / L$ values fall below the simulated curve, unlike the rest of the data. These are 130607-RecA-T4-narrow-9 ($L/l_P = 6.83$), 130607-RecA-T4-narrow-10 ($L/l_P = 10.62$), and 130905-RecA-T4-narrow-7 ($L/l_P = 13.28$); please refer to the corresponding kymographs at the end of this document, as well as the discussion here. Moreover, 130924-RecA-lambda-wide-2 ($L/l_P = 20.30$) appears interesting, since it is a long molecule which seems naturally to adopt a much more folded configuration in the 3000nm channel than the 2400nm channel; however, it appears to display a 'knot' (see figure above) in many of the microscopy frames.

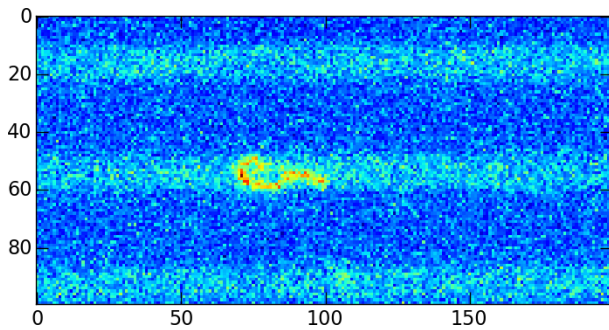


Figure 4: 130607-RecA-T4-narrow-9 ($L/l_P = 6.83$) at the start of the 1800nm channel sequence

130607-RecA-T4-narrow-9 ($L/l_P = 6.83$) is folded at the beginning of the 1800nm sequence, but it is not clear if this is an experimental error, or a natural back-fold. The molecule does seem to unfold around frame 138 of that sequence, with the folded end tumbling over the rest of the molecule until the left and right ends have switched and the molecule is extended. However, at around frame 210, the originally folded end once more folds back up against the rest of the molecule. At the beginning of the 2400nm sequence, the molecule appears quite tangled, and similar patterns are displayed for the rest of the experiment.

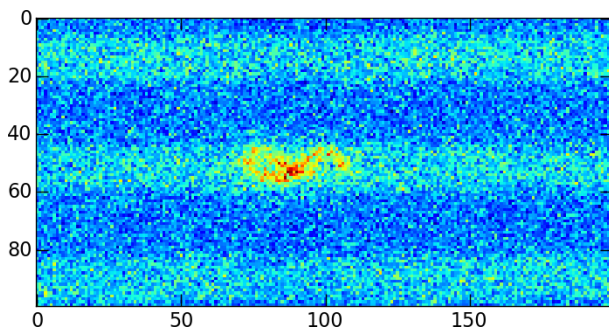


Figure 5: 130607-RecA-T4-narrow-10 ($L/l_P = 10.62$) at the start of the 2400nm channel sequence

130607-RecA-T4-narrow-10 ($L/l_P = 10.62$) is folded at the beginning of the 2400nm sequence,

but unfurls beginning at around frame 175, and remains without back-folds for the rest of the sequence. At the beginning of the 3000nm sequence, it is again completely folded over, and remains at least slightly folded for the rest of the sequence. It is not clear if this is due to experimental error.

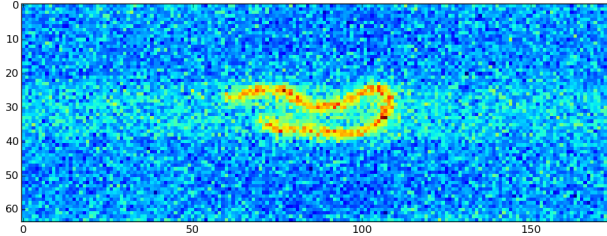


Figure 6: 130905-RecA-T4-narrow-7 ($L/l_P = 13.28$) at the start of the 2400nm channel sequence

Similarly, 130905-RecA-T4-narrow-7 ($L/l_P = 13.28$) is folded over at the beginning of the 2400nm sequence (the smallest channel for which we have data for this molecule), but it never seems to unfurl completely for the rest of the experiment.

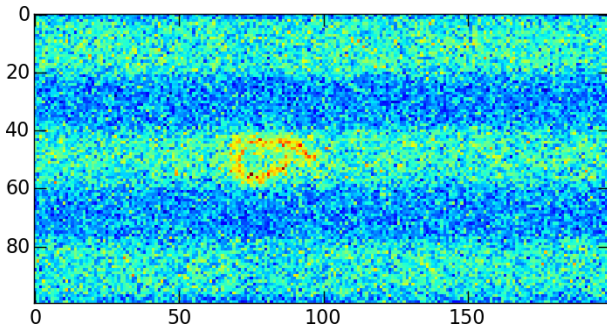


Figure 7: 130607-RecA-T4-wide-4 ($L/l_P = 8.35$) at frame 141 in the 3000nm channel

Finally, 130607-RecA-T4-wide-4 ($L/l_P = 8.35$; and which, like all experiments tagged 'wide', starts from the 3000nm channel, and moves to progressively narrower ones) folds over beginning around frame 110, unfolds substantially around frame 300, and then curls back up for the remainder of the time in that channel. A similar bimodal pattern is evident in the 2400nm channel. However, at the beginning of the 1800nm channel, one end is folded back slightly, which may be due to experimental error in the transition between channels. The molecule nonetheless unfolds at around frame 335.

130607-RecA-T4-wide-4 is the one of few molecules which seem to show clearly, particularly here in the two widest channels, a coherent folded configuration that mostly does not seem to be the result of an external experimental condition. Since it shows at least two modes of configuration – folded and unfolded – the average $\langle X \rangle$ is skewed accordingly, and hence this molecule is one of few that is consistent with the simulations. Note that its mean $\langle X \rangle/L$ values fall close to the simulated data (despite the large standard error).

2.1 Conclusions and further questions

We believe that the discrepancy presented here is a consequence of the conformational kinetics. The microscopy videos record at most 45 seconds which, given the frequency of conformational changes seen in the kymographs, is inadequate to obtain statistics in agreement with the equilibrium distributions simulated by Dorfman; moreover, only approximately ten seconds is taken after moving a molecule into a given channel and before starting the data collection, which is likely insufficient for the molecule to reach equilibrium. This analysis seems to be in agreement with

the form of the simulated distributions (not shown), which generally have a long tail that is not sampled here.

The classification of conformations and experimental conditions given below seems to support these conclusions. In particular, we see that, even in the widest (3000nm) channel, folds that change the extension of the molecule occur only 0.53 times every 100 frames on average. Most of the recordings show no folding, and an initial condition that does not indicate significant experimental influence.

2.2 Plots for each channel separately; both DNA types

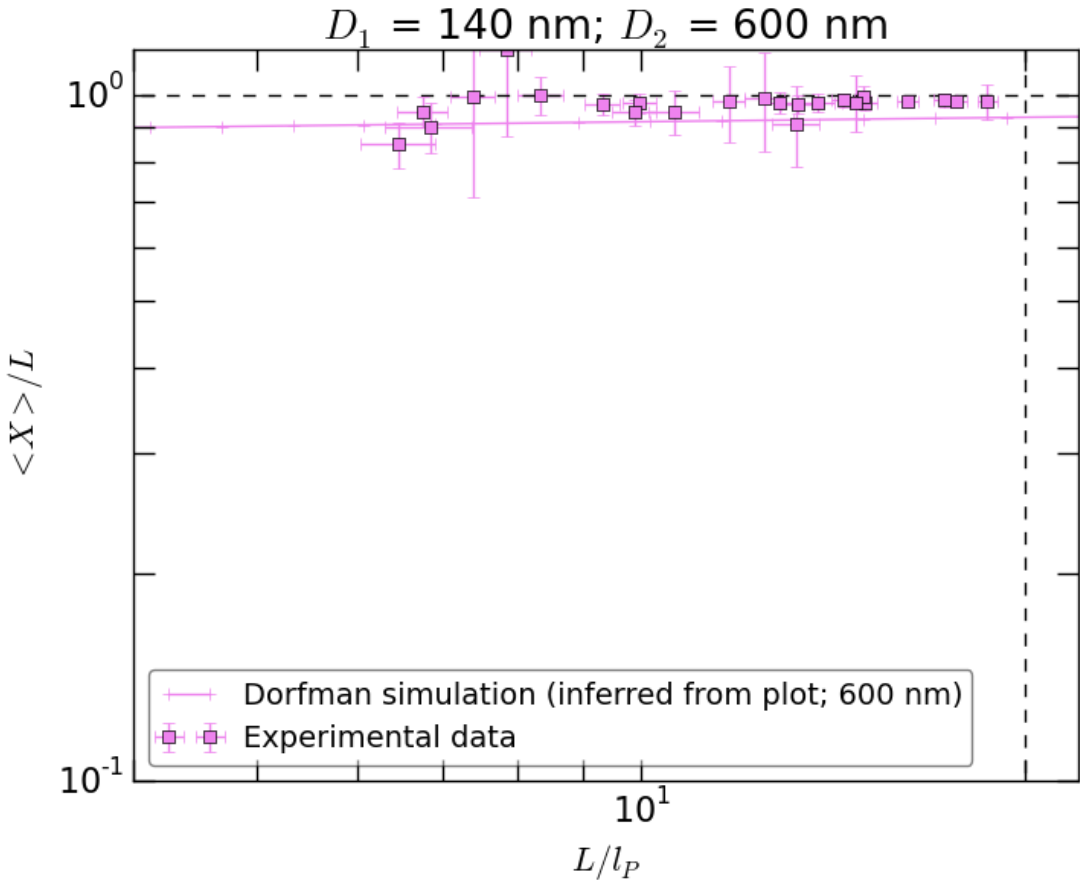


Figure 8: 600nm channel; log axes. The dashed vertical line is the dashed line in 2. Error bars represent one standard deviation.

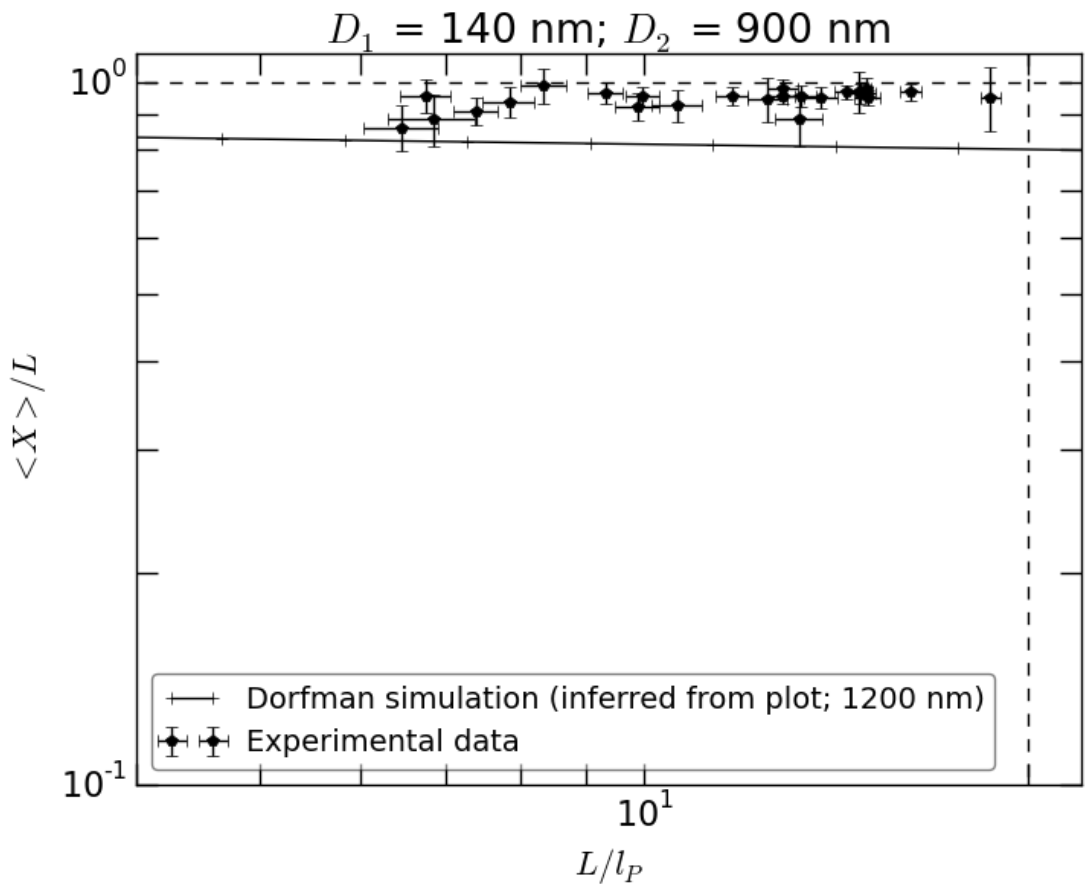


Figure 9: 900nm channel; log axes. Points represent experimental data, whilst the line represents the rescaled simulated data for the 1200nm channel. The dashed vertical line is the dashed line in 2. Error bars represent one standard deviation.

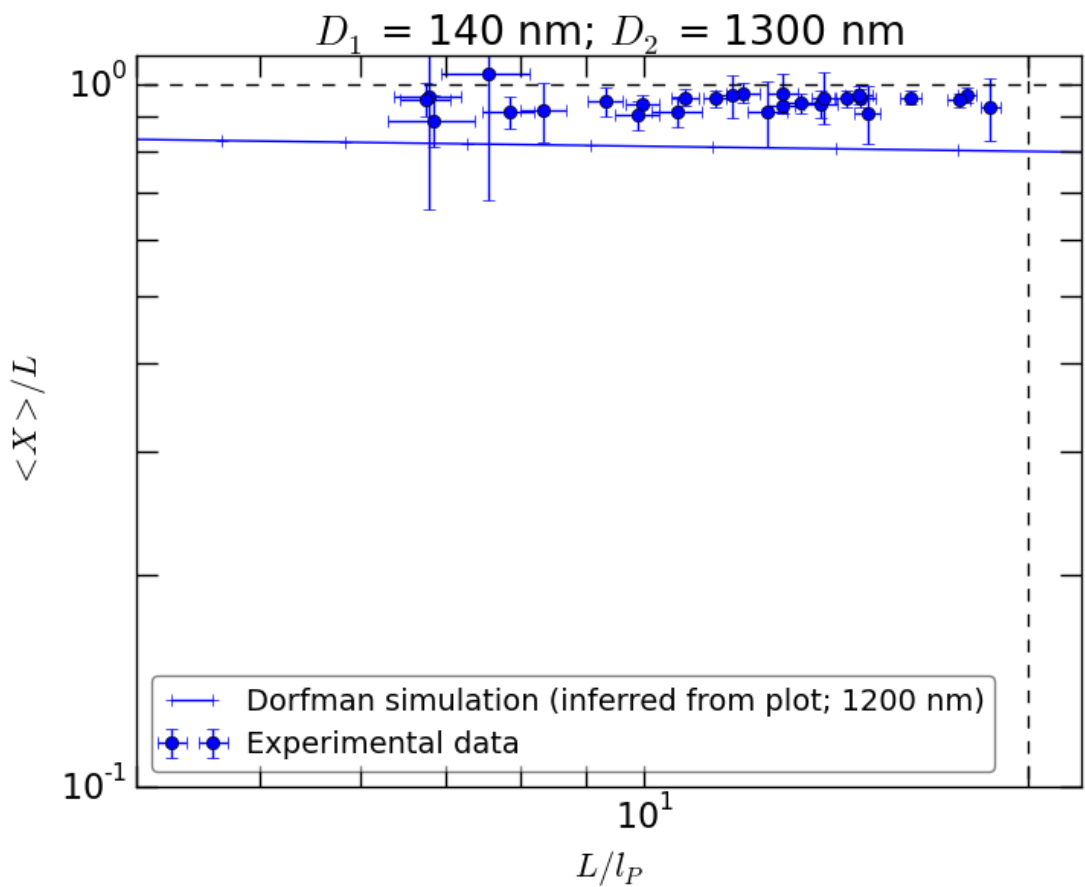


Figure 10: 1300nm channel; log axes. Points represent experimental data, whilst the line represents the rescaled simulated data for the 1200nm channel. The dashed vertical line is the dashed line in 2. Error bars represent one standard deviation.

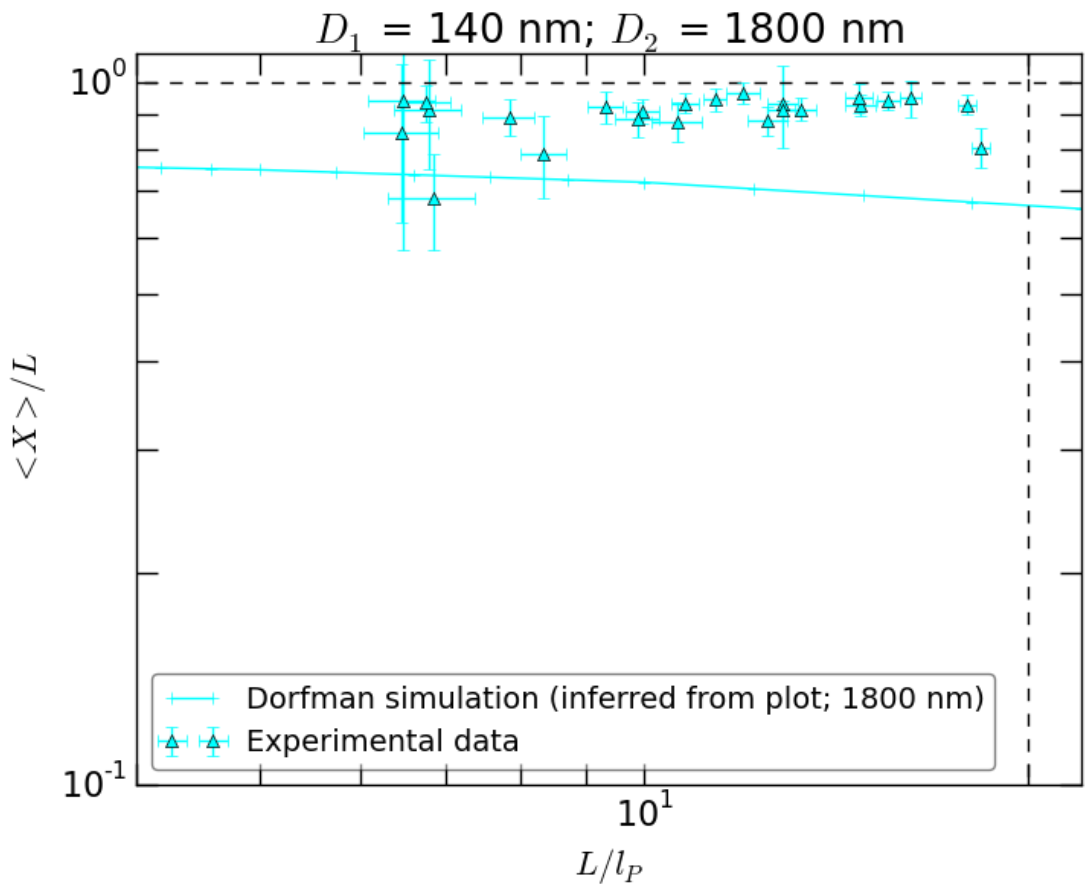


Figure 11: 1800nm channel; log axes. Points represent experimental data, whilst the line represents the rescaled simulated data for the 1800nm channel. The dashed vertical line is the dashed line in 2. Error bars represent one standard deviation. The point with lowest $\langle X \rangle / L$ value is 130607-RecA-T4-narrow-9 ($L / l_P = 6.83$), which was discussed above.

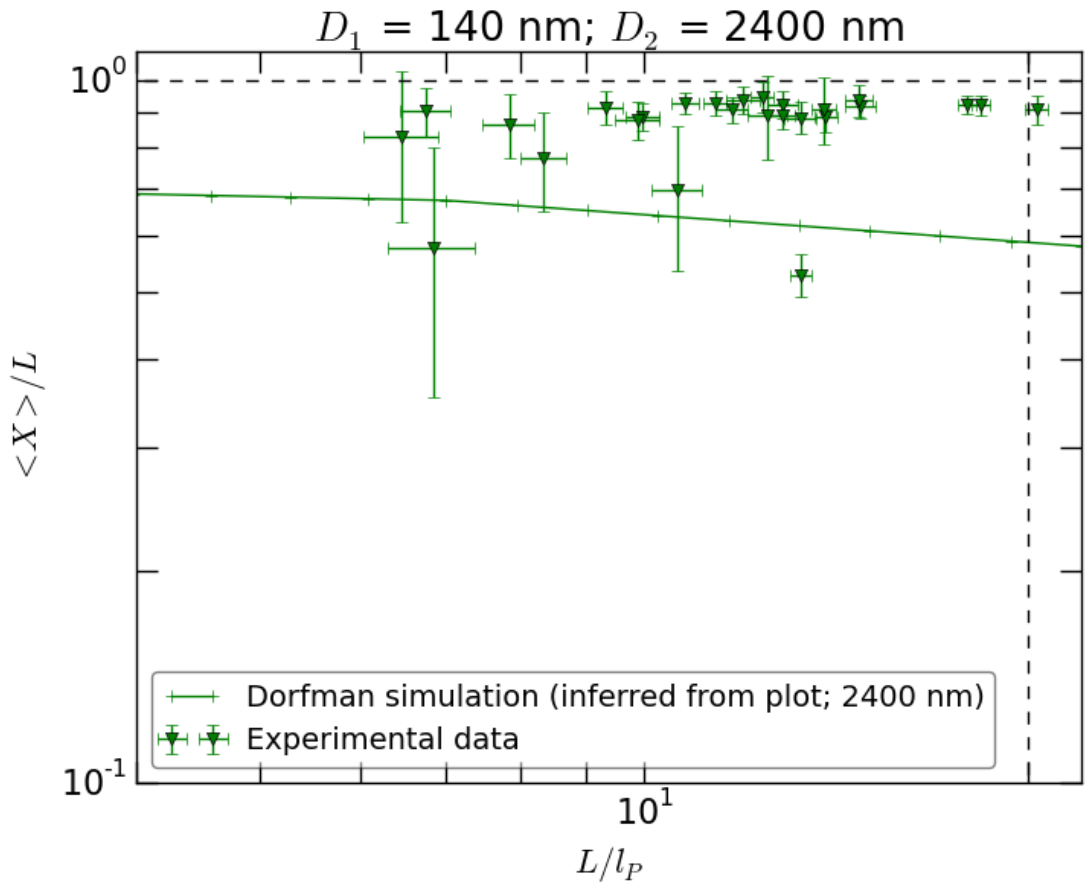


Figure 12: 2400nm channel; log axes. Points represent experimental data, whilst the line represents the rescaled simulated data for the 2400nm channel. The dashed vertical line is the dashed line in 2. Error bars represent one standard deviation. The two lower values are 130607-RecA-T4-narrow-9 ($L/l_P = 6.83$) and 130905-RecA-T4-narrow-7 ($L/l_P = 13.28$); they were discussed above.

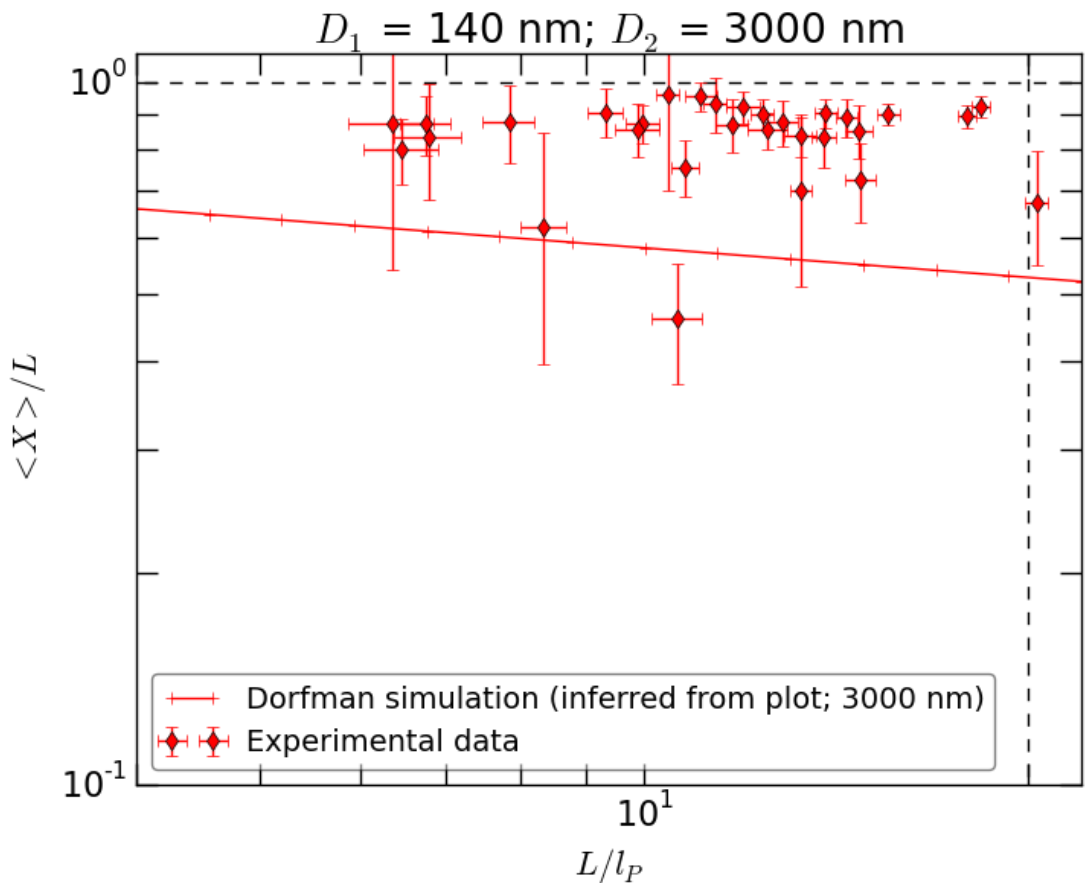


Figure 13: 3000nm channel; log axes. Points represent experimental data, whilst the line represents the rescaled simulated data for the 3000nm channel. The dashed vertical line is the dashed line in 2. Error bars represent one standard deviation. The point with lowest $\langle X \rangle / L$ value is 130607-RecA-T4-narrow-10 ($L/l_p = 10.62$), which was discussed above.

2.3 Plots for T4 DNA only

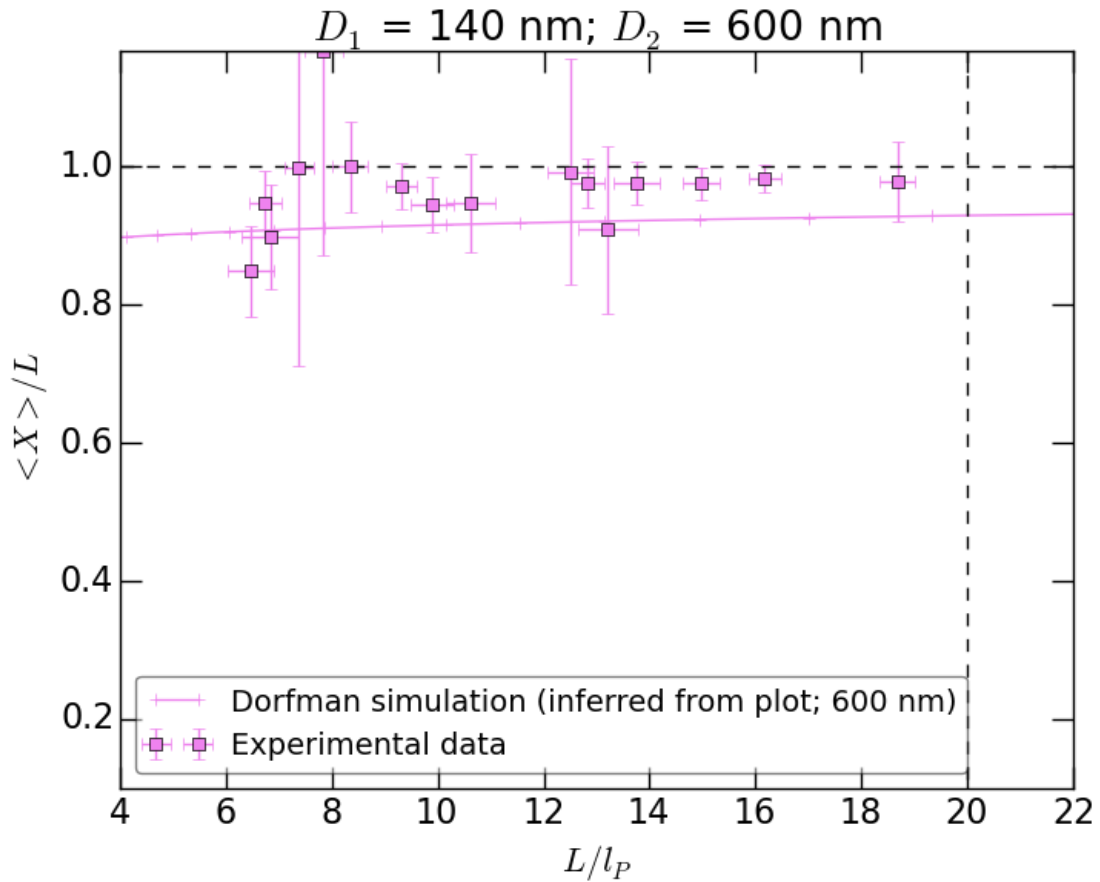


Figure 14: 600nm channel; linear axes. The dashed vertical line is the dashed line in 2. Error bars represent one standard deviation.

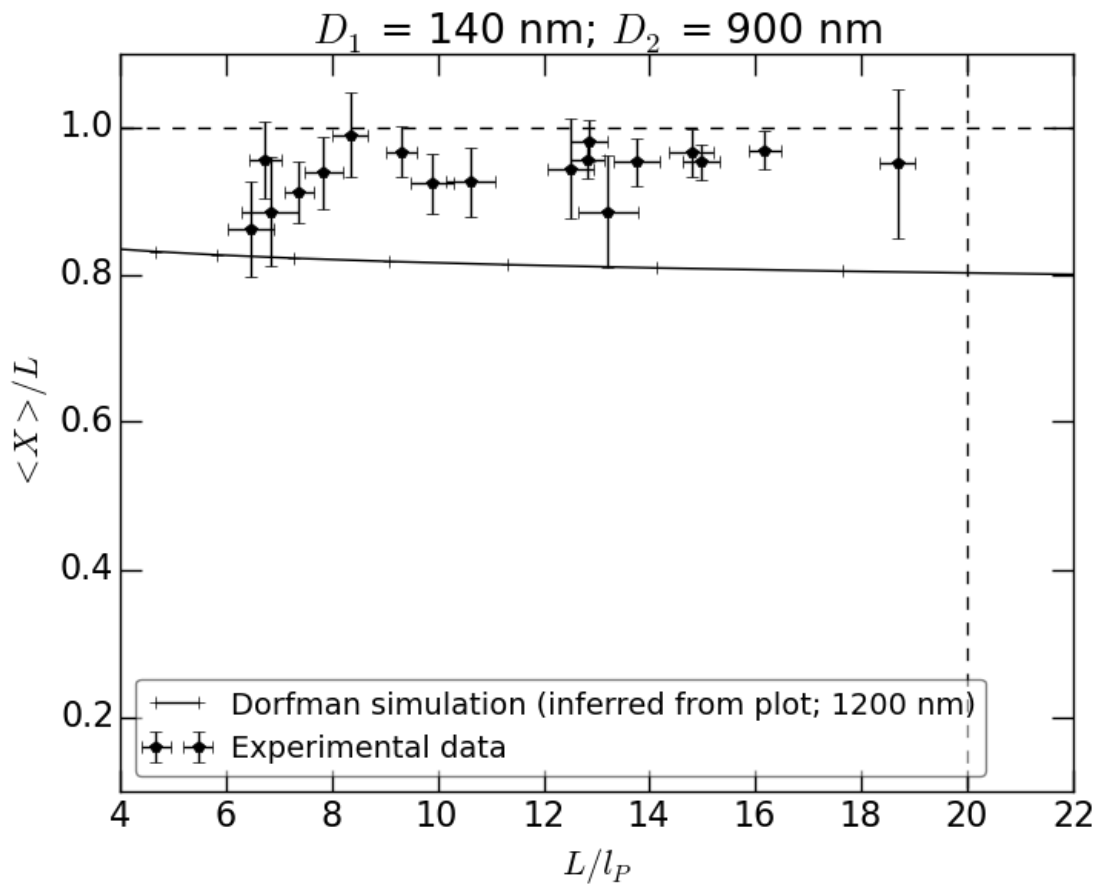


Figure 15: 900nm channel; linear axes. Points represent experimental data, whilst the line represents the rescaled simulated data for the 1200nm channel. The dashed vertical line is the dashed line in 2. Error bars represent one standard deviation.

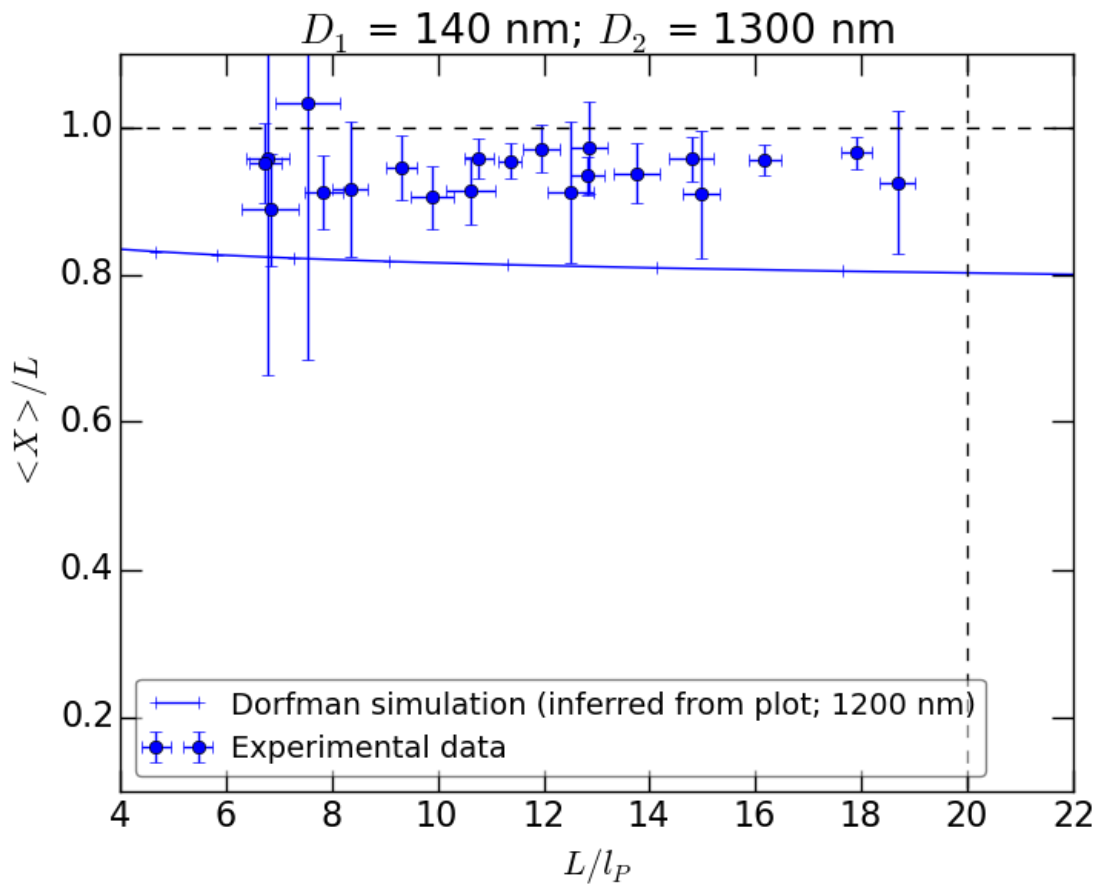


Figure 16: 1300nm channel; linear axes. Points represent experimental data, whilst the line represents the rescaled simulated data for the 1200nm channel. The dashed vertical line is the dashed line in 2. Error bars represent one standard deviation.

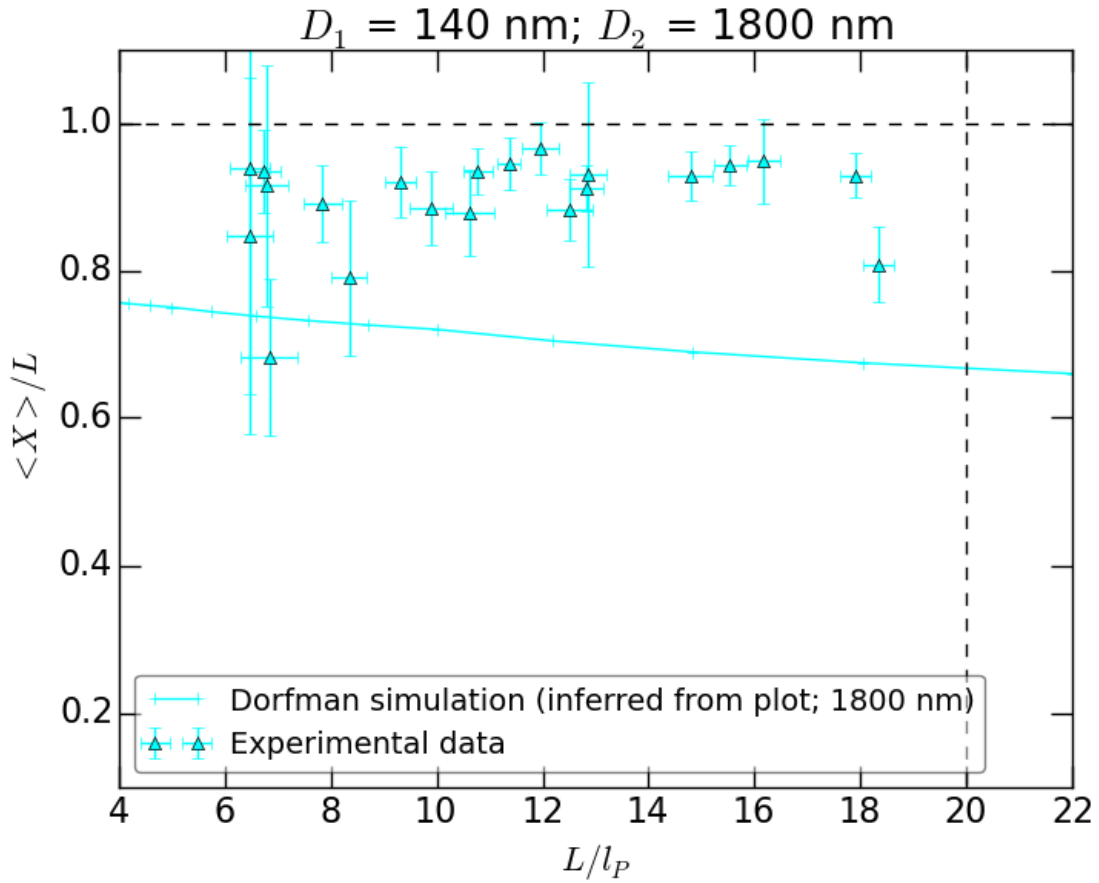


Figure 17: 1800nm channel; linear axes. Points represent experimental data, whilst the line represents the rescaled simulated data for the 1800nm channel. The dashed vertical line is the dashed line in 2. Error bars represent one standard deviation. The point with lowest $\langle X \rangle / L$ value is 130607-RecA-T4-narrow-9 ($L / l_P = 6.83$), which was discussed above.

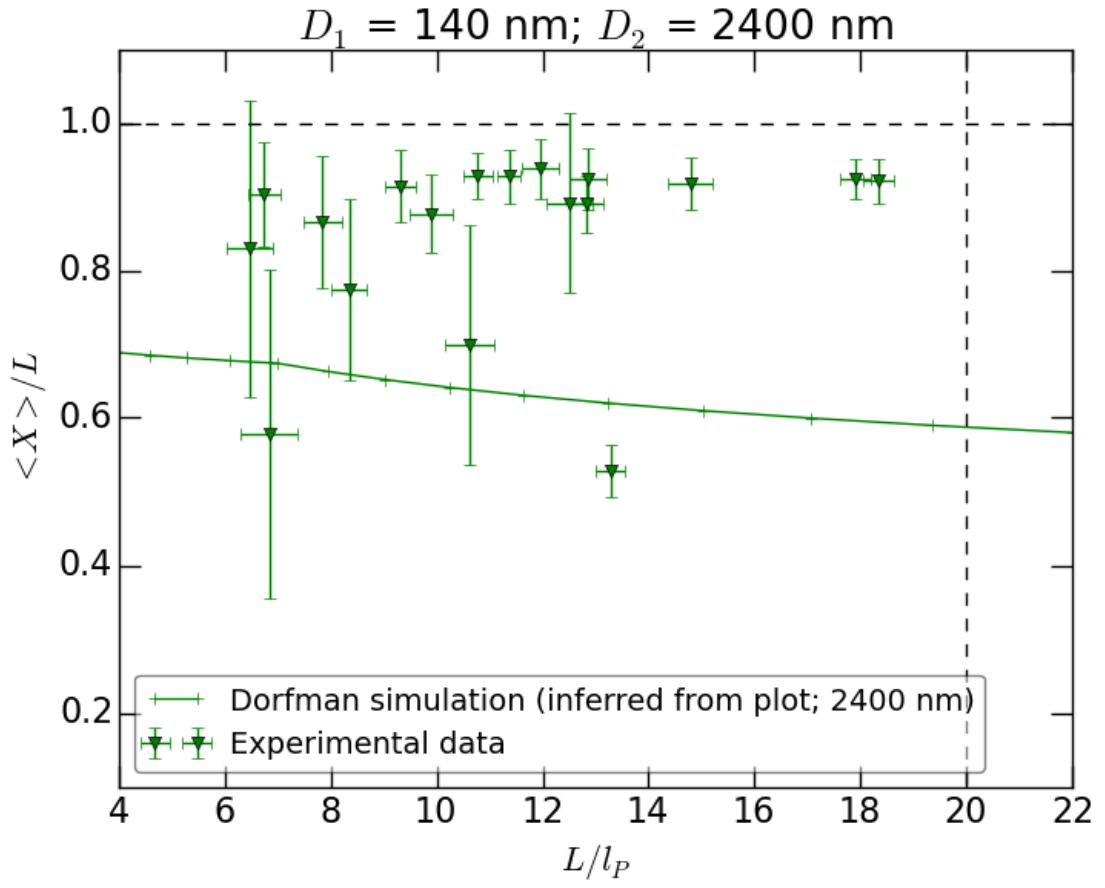


Figure 18: 2400nm channel; linear axes. Points represent experimental data, whilst the line represents the rescaled simulated data for the 2400nm channel. The dashed vertical line is the dashed line in 2. Error bars represent one standard deviation. The two lower values are 130607-RecA-T4-narrow-9 ($L/l_P = 6.83$) and 130905-RecA-T4-narrow-7 ($L/l_P = 13.28$); they were discussed above.

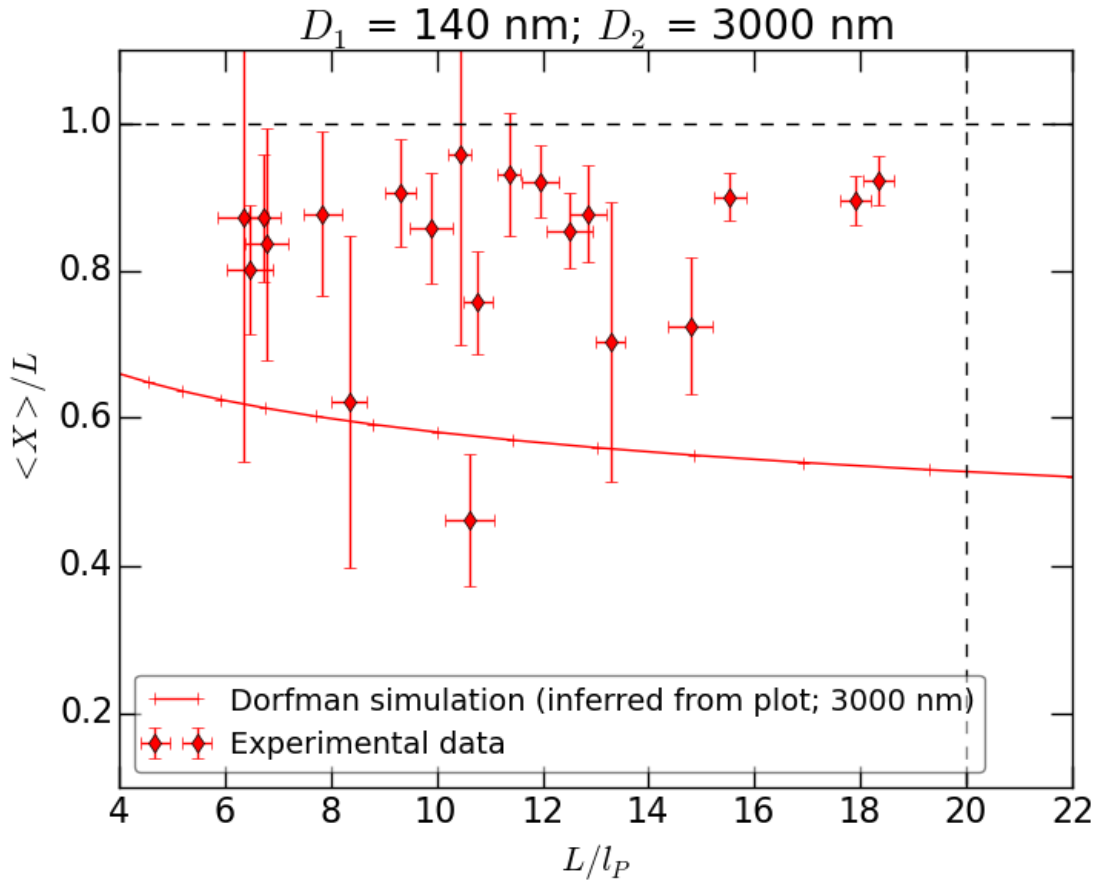


Figure 19: 3000nm channel; linear axes. Points represent experimental data, whilst the line represents the rescaled simulated data for the 3000nm channel. The dashed vertical line is the dashed line in 2. Error bars represent one standard deviation. The point with lowest $\langle X \rangle / L$ value is 130607-RecA-T4-narrow-10 ($L / l_P = 10.62$), which was discussed above.

2.4 Plots for λ DNA only

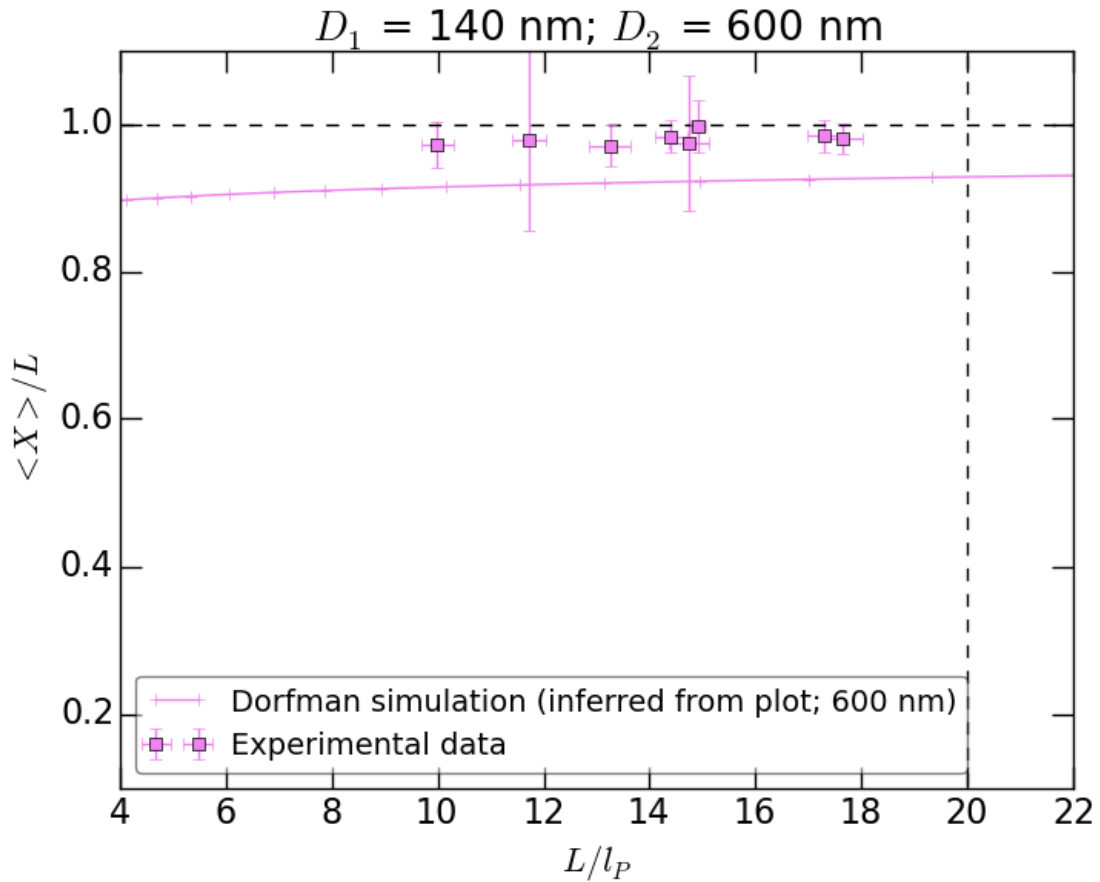


Figure 20: 600nm channel; linear axes. The dashed vertical line is the dashed line in 2. Error bars represent one standard deviation.

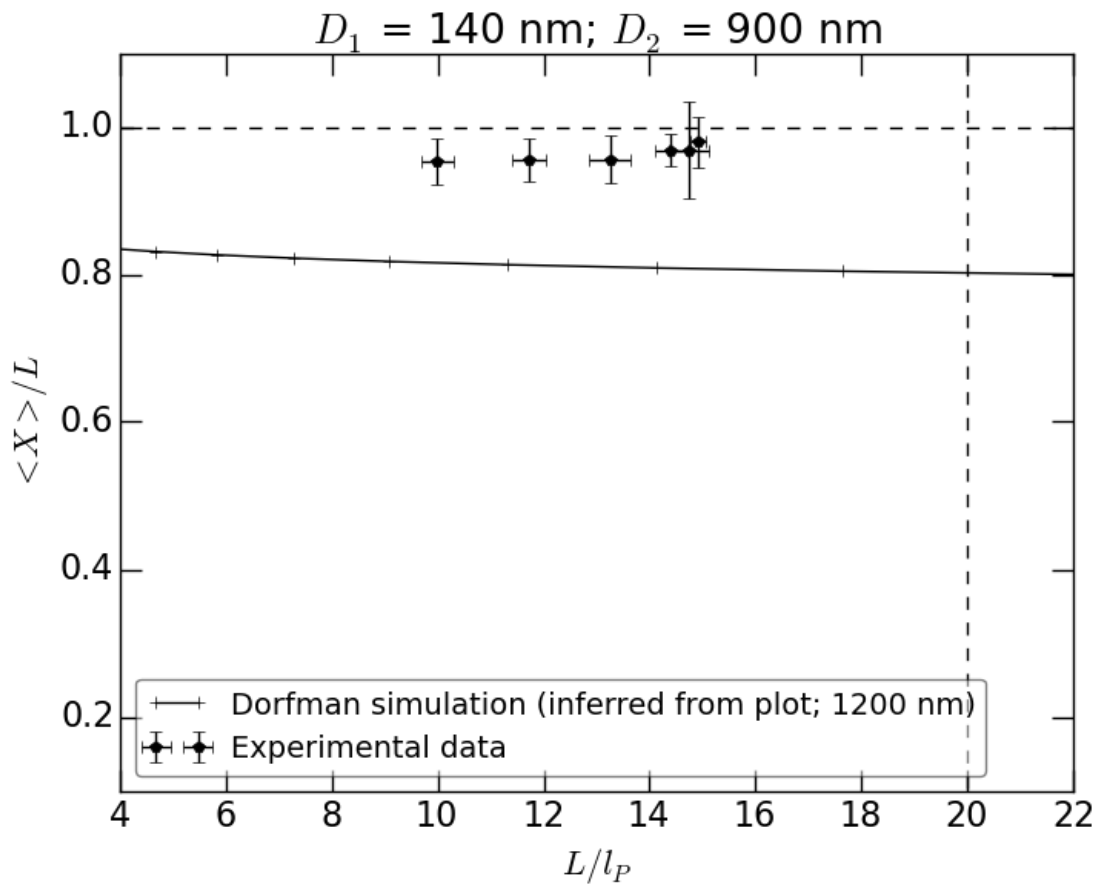


Figure 21: 900nm channel; linear axes. Points represent experimental data, whilst the line represents the rescaled simulated data for the 1200nm channel. The dashed vertical line is the dashed line in 2. Error bars represent one standard deviation.

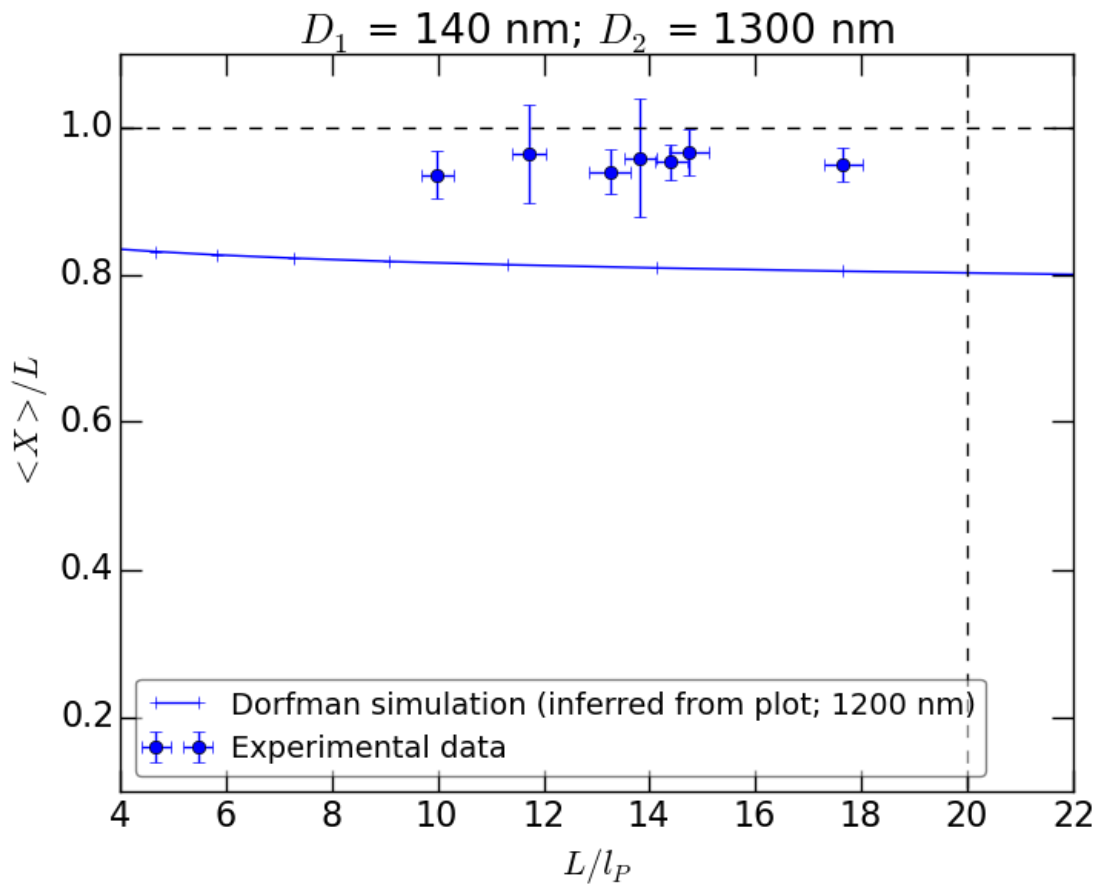


Figure 22: 1300nm channel; linear axes. Points represent experimental data, whilst the line represents the rescaled simulated data for the 1200nm channel. The dashed vertical line is the dashed line in 2. Error bars represent one standard deviation.

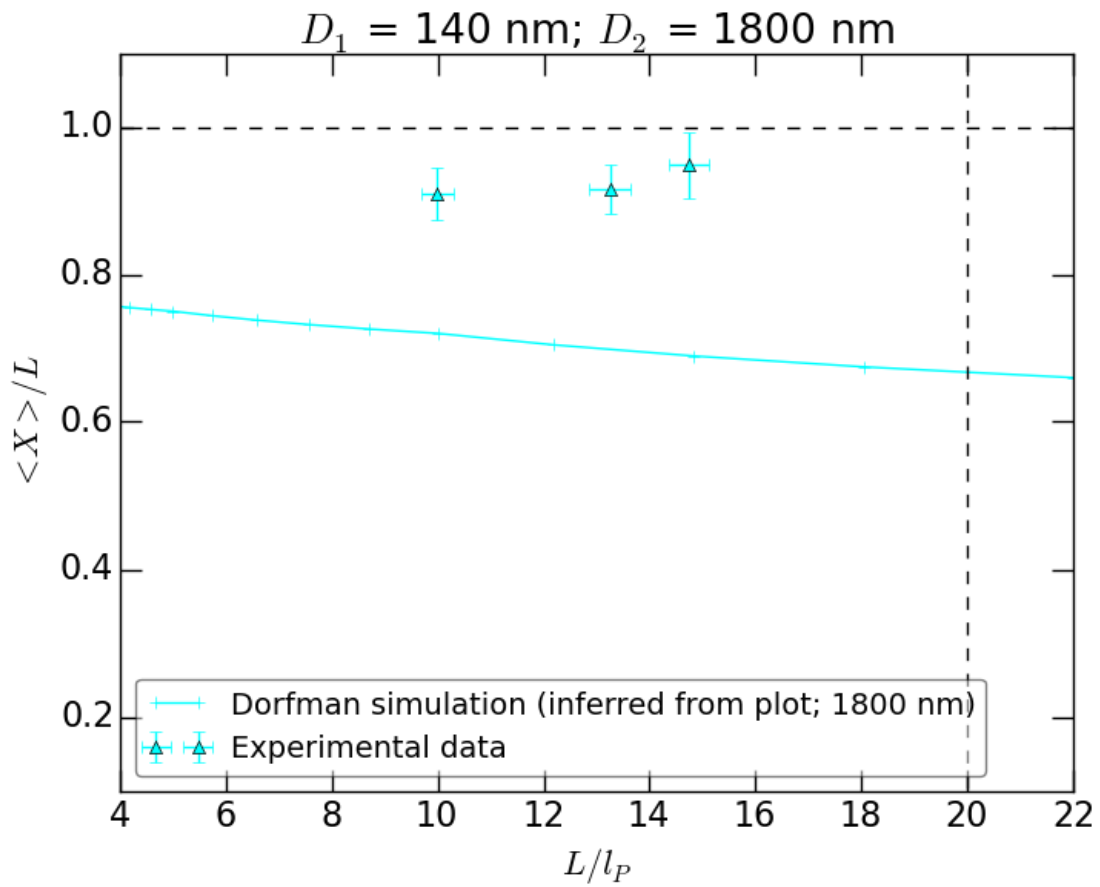


Figure 23: 1800nm channel; linear axes. Points represent experimental data, whilst the line represents the rescaled simulated data for the 1800nm channel. The dashed vertical line is the dashed line in 2. Error bars represent one standard deviation.

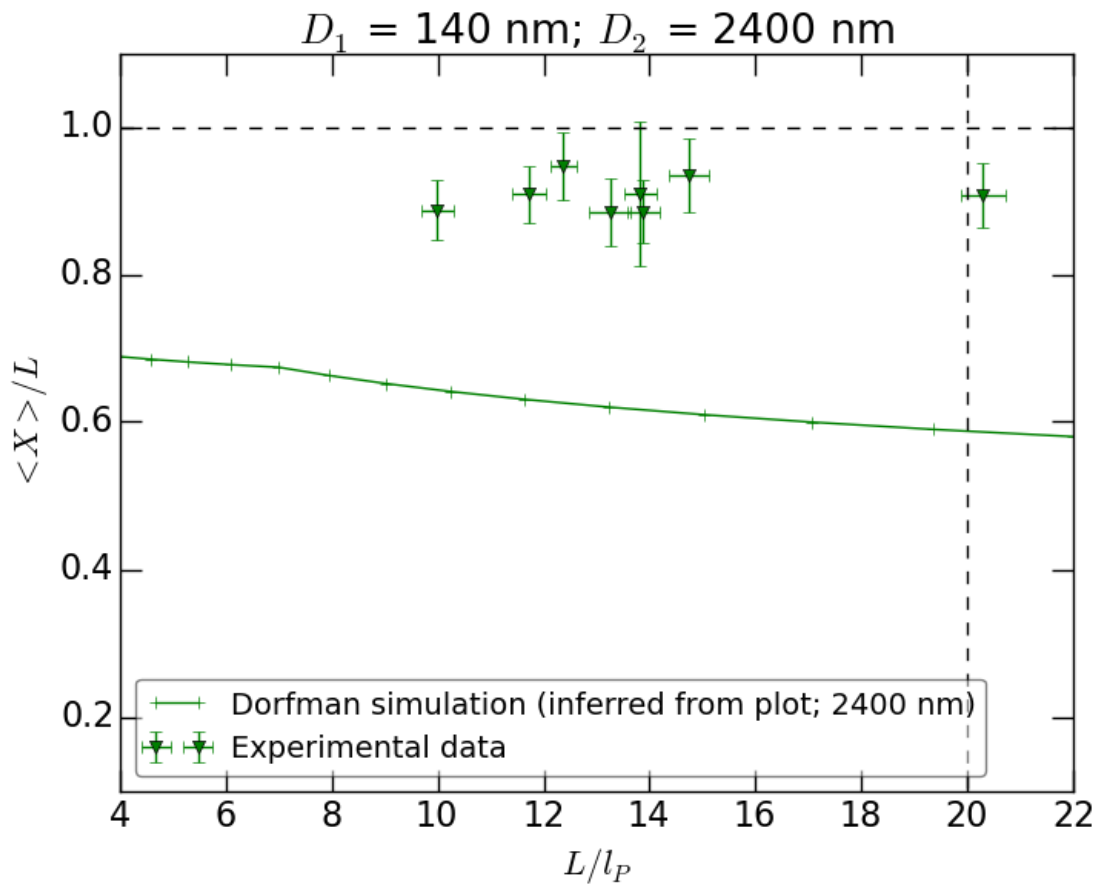


Figure 24: 2400nm channel; linear axes. Points represent experimental data, whilst the line represents the rescaled simulated data for the 2400nm channel. The dashed vertical line is the dashed line in 2. Error bars represent one standard deviation.

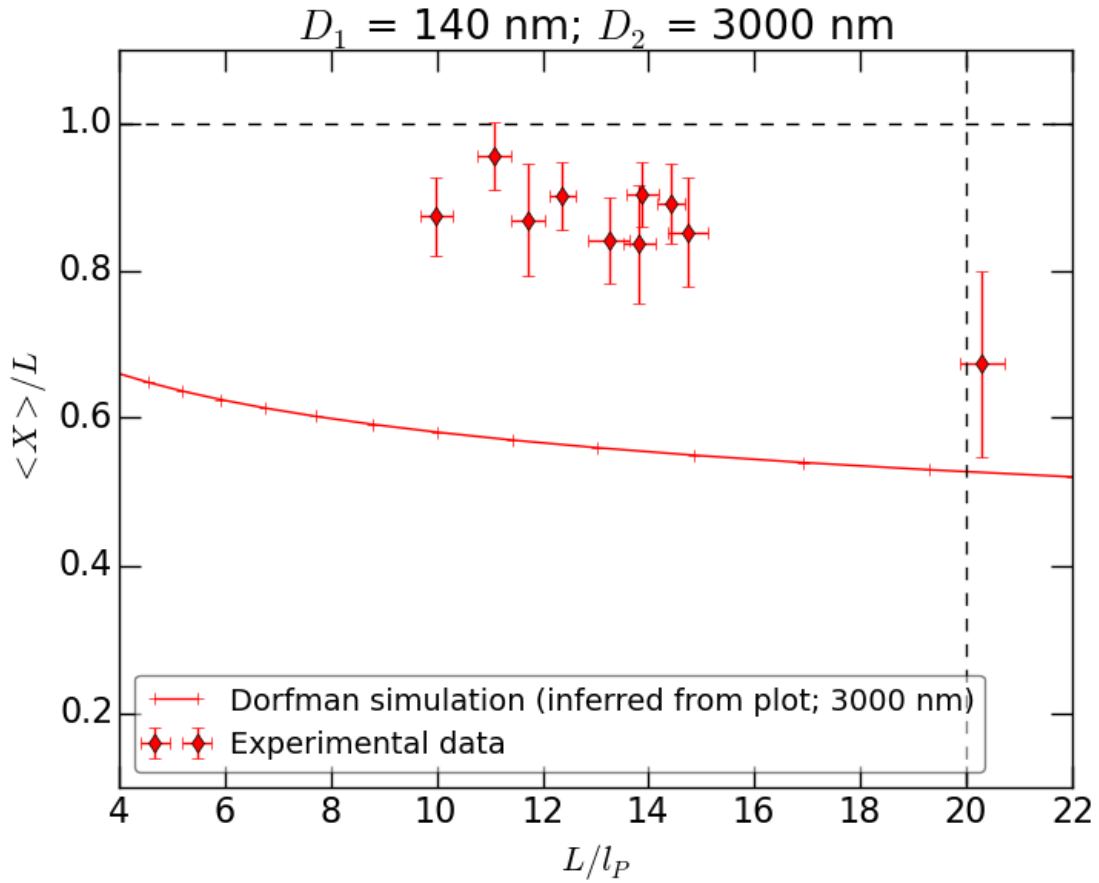


Figure 25: 3000nm channel; linear axes. Points represent experimental data, whilst the line represents the rescaled simulated data for the 3000nm channel. The dashed vertical line is the dashed line in 2. Error bars represent one standard deviation.

2.5 Rejected configurations

130607-RecA-T4-narrow-8 ($L/l_P = 13.22$, not shown) is folded over or knotted at the beginning of the 1300nm sequence, and never unfolds throughout the rest of the experiment. It seems highly likely that this is an experimental error, as there is little change in the conformation from this point on. The error can arise when the molecule transitions between channels of different widths, getting tangled in the process; in the experiments tagged 'narrow', the molecules start at the narrowest channel, moving to wider channels, whilst in those experiments tagged 'wide', the reverse occurs. Once a molecule becomes tangled in this way, it often does not untangle at any point in the rest of the experiment.

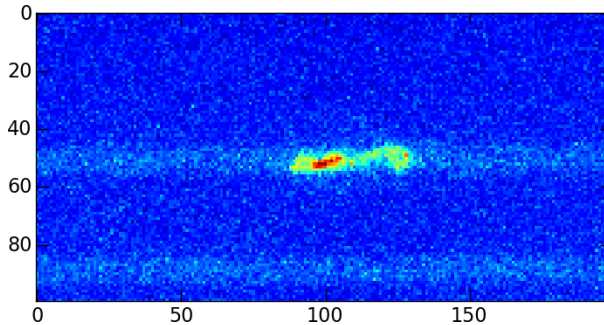


Figure 26: 130607-RecA-T4-narrow-8 at the start of the 1300nm channel sequence

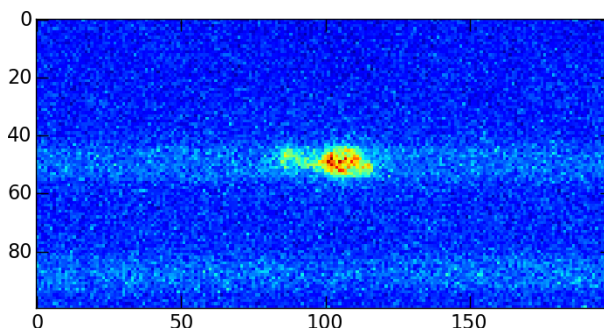


Figure 27: 130607-RecA-T4-narrow-8 at the start of the 1800nm channel sequence

Similarly suspicious experimental conditions are visible in the following cases: 130905-RecA-T4-narrow-3 (1800nm), 130905-RecA-T4-narrow-4 (1800nm), 130905-RecA-T4-wide-3 (600nm and 900nm), 130905-RecA-T4-wide-7 (600nm), 130905-RecA-T4-wide-8 (1300nm), and 130924-RecA-lambda-wide-3 (2400nm).

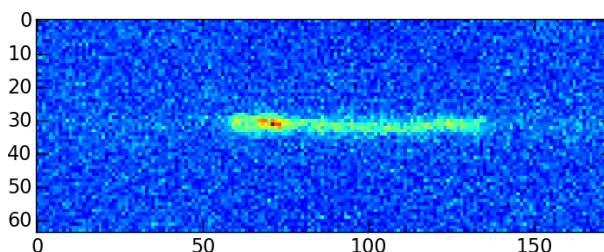


Figure 28: 130605-RecA-T4-wide-7 at the start of the 600nm channel sequence

The following points were rejected because their relative $\langle X \rangle / L$ errors exceeded the 0.4 threshold: 130603-RecA-T4-wide-4 (0.48 at 1800 nm, 0.59 at 2400 nm); 130603-RecA-T4-wide-3 (0.65 at 2400 nm); 130603-RecA-T4-wide-2 (0.53 at 2400 nm, 0.73 at 3000 nm); 130607-RecA-T4-wide-1 (0.67 at 1300 nm); 130607-RecA-T4-narrow-9 (0.61 at 3000 nm); and 130603-RecA-T4-wide-5 (0.55 at 1800 nm, 0.40 at 2400 nm, 0.53 at 3000 nm).

3 Classification of conformations and experimental conditions

3.1 Summary

3.1.1 Main findings

- The initial conditions can have a large effect on the conformations adopted, but in the majority of cases, there is no unusual initial condition.
- There is a preference for unfolded conformations, followed by equal numbers of instances of folding and unfolding, followed by more unfolding than folding (where the initial condition was folded but not stuck).
- Most of the folding occurs in the widest channels, but even at 3000 nm, only 0.53 extension-changing folds every 100 frames on average.
- Moving from a wide channel to a narrow channel is more likely to produce an experimental error than vice versa, although “stuck” ends are not significantly more likely in either direction.
- In most cases, there is some drift of the molecules in the channel, probably resulting from unequal pressure. But also in most cases, there is no folding.
- Where there is folding, there is an effect of drift on folding, particularly when the drift is aligned with the direction of movement from channel to channel, such that the conformations produced tend to align with the drift and channel movement.

3.1.2 Notes on experimental conditions

Firstly, there was no systematic timing in the experiments, and in particular, no systematic equilibration time before starting recording, after moving each molecule into its channel.

Secondly, there was on some unknown occasions “pressure leakage” in the channels, and attempts were made at compensating for this by applying pressure in the opposing direction in the channel; therefore, the pressure in the channels was not necessarily in equilibrium, and sometimes drift of the molecule is recorded in the videos. It is not clear what proportion of the drift is explained in this way.

Thirdly, on some unknown occasions, where “irreversible folds” (suspected to be experimentally induced) were noticed in the molecules, it was attempted to unfold the molecule by moving it “back and forth” in the channel. It is not clear where this occurred, or whether it occurred during or prior to recording.

3.1.3 How does the initial condition affect the subsequent conformations?

Most of the initial conditions are ~ (see Table 1 for explanation of these conformation symbols). Where the initial conditions are not ~, the initial condition only seems to affect the subsequent conformation if it involves “stuck” folded ends (ie, those that somehow seem to have become glued to the bulk of the filament).

The following cases show stuck ends:

- 130607-RecA-T4-narrow-8 (at 1300 nm and subsequently 1800nm)
- 130905-RecA-T4-narrow-3 (at 1800nm – the last width for which we have data)
- 130905-RecA-T4-narrow-4 (at 1800nm – the last width for which we have data)
- 130905-RecA-T4-narrow-7 (at 3000nm)
- 130905-RecA-T4-wide-3 (at 900 nm and subsequently 600 nm – but not at the “front” end)

- 130905-RecA-T4-wide-7 (at 600 nm – again not at the “front” end)
- 130924-RecA-lambda-wide-3 (at 2400 nm – the last width for which we have data)

The following cases show unusual initial conditions that do not include stuck ends:

- 130607-RecA-T4-narrow-9 (initially folded front at 1800 and 2400nm, which later unfolds)
- 130607-RecA-T4-wide-4 (an initially folded front end at 1800 nm that later unfolds)
- 130905-RecA-T4-wide-2 (a bright “clump” visible at the front end throughout all the recordings)
- 130905-RecA-T4-wide-8 (a point on filament around which bending is easier; perhaps a gap in the protein coating?)
- 130924-RecA-lambda-wide-4 (a loop is visible from the start at 3000 nm)
- 130924-RecA-lambda-wide-8 (a loop is visible from 2400 nm through 1800 nm, but not thereafter)

3.1.4 Are (experimentally-induced) stuck ends more likely wide to narrow or vice versa?

Neither direction of movement is more likely to produce “stuck” folded ends. Looking again at the cases detailed above, we have 4 cases of stuck ends when moving from narrow to wide, and 3 cases of stuck ends when moving from wide to narrow. But there are 5 other wide-to-narrow experimental oddities, against just 1 for narrow-to-wide, which suggests that wide-to-narrow is nonetheless more likely to produce experimental error during the progression of the experiment.

3.1.5 Do folds preferentially form in the direction of the drift, or of the movement from channel to channel?

In most cases, there is some drift of the molecule in the channel, and no folding. Sometimes, the drift seems obviously to affect folding, as in the case of 130607-RecA-T4-narrow-10 (unfolding at 2400 nm due to channel pressure change; initial condition is folded in direction of movement) or 130603-RecA-T4-wide-5 (folds occur when drift is 0, preferentially in direction of movement). Where the initial condition is folded, it is more often the case that this folding is in the direction of movement (9 vs 6 cases), but it is hard to say if this is a significant difference.

The remaining, spontaneous, cases are detailed in Table 2. We see that, where there is no drift, there is no preference for folding to occur in either direction. Where there is a forwards drift (ie, in the direction of movement from channel to channel), there is a preference for folding also in the forwards direction. Finally, where there is a backwards drift (against the direction of movement from channel to channel), there is still a slight preference for folding in the forwards direction (opposed to the drift). This suggests that there is only an effect of drift on the direction of spontaneous folding when the drift is in the direction of channel movement.

3.1.6 Which is faster or more likely, folding or unfolding?

There is clearly a preference for unfolded configurations, except where folding is apparently induced by experimental conditions. Most recordings show no folding at all. Of the remainder, there is a preference for equal numbers of folding and unfolding (15 cases), followed by more unfolding (7 cases), and finally, there are only 4 cases where the recordings show more folding than unfolding. The cases of more unfolding are explained by their having a folded initial condition. There is no difference between the speed at which conformations change from folded to unfolded or vice versa, except in the cases where the initial condition has “stuck” folded ends, in which cases unfolding at the ends does not occur.

3.1.7 How do the fold rates vary with channel width?

Ignoring the effect of contour length on the fold rate, the average fold rates for the different channel widths are: 0.00 at 600 and 900 nm; 0.01 at 1300 nm; 0.05 at 1800 nm; 0.19 at 2400 nm; and 0.53 at 3000 nm. Clearly, as expected, most of the folding happens in the largest channels.

3.2 Tables

In the tables below, fold rate means the number of changes in conformation, per 100 frames, that cause a significant change in the extension of the molecule.

The average fold rates for the different channel widths are: 0.00 at 600 and 900 nm; 0.01 at 1300 nm; 0.05 at 1800 nm; 0.19 at 2400 nm; and 0.53 at 3000 nm.

The drift and fold direction give the direction of any drift of the filament in the channel, and the alignment of folded conformations (such as 'U') with the movement from channel to channel. Therefore, in both cases, 'forwards' means with the direction of travel from channel to channel, and 'backwards' means against the direction of travel. 'None' means there is no drift or folding. 'Neither' means that there are folded conformations but that they are not aligned with the movement in either direction. 'Both' means there is drift or there are folds in both directions.

Finally, the symbols describing the conformations of the filament are explained in the table below.

Table 1: Legend for conformation symbols

Symbol	Explanation
\sim	Small fluctuations along the length of the filament, with the filament aligned with the channel.
\curvearrowleft	Fewer, larger fluctuations along the length of the filament, like an 'S' on its side, aligned with the channel.
S	An 'S' shape, perpendicular to the length of the channel.
U	A single U bend, perpendicular to the length of the channel.
\cap	A single \cap bend, perpendicular to the length of the channel.
Ω	A bend in the form of an ' Ω '.
\supset	A single \supset bend, aligned with the length of the channel.
\subset	A single \subset bend, aligned with the length of the channel.
\bowtie	Like the \bowtie symbol: a bend aligned with the length of the channel, but with ends crossed over each other.
$\bowtie\bowtie$	Like \bowtie , but with ends not quite crossed over, and of asymmetric lengths.
σ	A curl in the left end of the filament, of the form of the symbol.
ϖ	A curl in the right end of the filament, of the form of the symbol.
ρ	A curl in the left end of the filament, of the form of the symbol.
ϱ	A curl in the right end of the filament, of the form of the symbol.
$\varpi\varpi$	A loop in the middle of the filament, apparently formed by the molecule crossing itself.

Table 2: Average fold rates for different directions of drift and channel movement, excluding cases of experimental oddity detailed above

Drift	Fold direction	Mean fold rate
None	Forwards	0.60
None	Backwards	0.70
None	Neither	0.25
Forwards	Forwards	1.25
Forwards	Backwards	0.25
Forwards	Neither	0.75
Backwards	Forwards	0.50
Backwards	Backwards	0.00
Backwards	Neither	0.81

Table 3: 130603-RecA-T4-wide-2. T4 DNA. Started at 3000 nm channel. $L/l_P = 6.47$

D	Initial condition	Fold rate	Drift	Fold direction
3000	U	0.75	None	Forwards
2400	~	0.25	Forwards	Backwards
1800	~	0	Forwards	None

Table 4: 130603-RecA-T4-wide-3. T4 DNA. Started at 3000 nm channel. $L/l_P = 6.79$

D	Initial condition	Fold rate	Drift	Fold direction
3000	~	0	Forwards	None
2400	~	0	Forwards	None
1800	~	0	Forwards	None
1300	~	0	Forwards	None

Table 5: 130603-RecA-T4-wide-4. T4 DNA. Started at 3000 nm channel. $L/l_P = 6.34$

D	Initial condition	Fold rate	Drift	Fold direction
3000	~	0	None	None
2400	~	0	Backwards	None
1800	~	0	Backwards	None

Table 6: 130603-RecA-T4-wide-5. T4 DNA. Started at 3000 nm channel. $L/l_P = 7.54$

D	Initial condition	Fold rate	Drift	Fold direction	Comments
3000	~	0.50	Backwards	Forwards	Folds occur when drift is 0
2400	~	0	Backwards	None	
1800	~	0	Backwards	None	
1300	~	0	Backwards	None	

Table 7: 130603-RecA-T4-wide-7. T4 DNA. Started at 3000 nm channel. $L/l_P = 12.50$

D	Initial condition	Fold rate	Drift	Fold direction	Comments
3000	~	0	None	None	
2400	~	0	Backwards	None	
1800	~	0	Backwards	None	
1300	~	0	Backwards	None	
900	~	0	Backwards	None	
600	~	0	Backwards	None	Drift not constant; pressure leakage?

Table 8: 130607-RecA-T4-narrow-10. T4 DNA. Started at 600 nm channel. $L/l_P = 10.62$

D	Initial condition	Fold rate	Drift	Fold direction	Comments
600	~	0	Forwards	None	
900	~	0	Both	None	
1300	~	0	None	None	
1800	~	0	Forwards	None	
2400	∞	1.00	Forwards	Forwards	Final unfolding occurs once drift begins. Suggests unfolding due to channel pressure change.
3000	σ	1.50	Forwards	Forwards	See previous comment.

Table 9: 130607-RecA-T4-narrow-7. T4 DNA. Started at 600 nm channel. $L/l_P = 7.38$

D	Initial condition	Fold rate	Drift	Fold direction
600	~	0	Forwards	None
900	~	0	Both	None

Table 10: 130607-RecA-T4-narrow-8. T4 DNA. Started at 600 nm channel. $L/l_P = 13.22$

D	Initial condition	Fold rate	Drift	Fold direction	Comments
600	~	0	Forwards	None	
900	~	0	Forwards	None	
1300	o..o	0	Forwards	Forwards	Suggests experimental error
1800	o	0	Forwards	Forwards	Suggests experimental error

Table 11: 130607-RecA-T4-narrow-9. T4 DNA. Started at 600 nm channel. $L/l_P = 6.83$

D	Initial condition	Fold rate	Drift	Fold direction	Comments
600	~	0	Forwards	None	
900	~	0	Both	None	
1300	~	0	Forwards	None	
1800	o	1.00	None	Neither	Initial fold in direction of channel movement.
2400	o	1.25	Backwards	Neither	Initial fold in direction of channel movement.
3000	~	0.50	Forwards	Forwards	But final configuration (\supset) does not point forwards.

Table 12: 130607-RecA-T4-wide-1. T4 DNA. Started at 3000 nm channel. $L/l_P = 6.46$

D	Initial condition	Fold rate	Drift	Fold direction	Comments
3000	S	0.25	None	Neither	Initial S becomes ~ by frame 5.
2400	~	0	None	None	
1800	~	0	None	None	
1300	~	0	Forwards	None	
900	~	0	None	None	
600	~	0	Forwards	None	

Table 13: 130607-RecA-T4-wide-2. T4 DNA. Started at 3000 nm channel. $L/l_P = 6.74$

D	Initial condition	Fold rate	Drift	Fold direction
3000	o	0.75	None	Forwards
2400	~	0	None	None
1800	~	0	None	None
1300	~	0	Backwards	None
900	~	0	Backwards	None
600	~	0	None	None

Table 14: 130607-RecA-T4-wide-3. T4 DNA. Started at 3000 nm channel. $L/l_P = 9.32$

D	Initial condition	Fold rate	Drift	Fold direction
3000	~	0	None	None
2400	~	0	None	None
1800	~	0	None	None
1300	~	0	None	None
900	~	0	None	None
600	~	0	Backwards	None

Table 15: 130607-RecA-T4-wide-4. T4 DNA. Started at 3000 nm channel. $L/l_P = 8.35$

D	Initial condition	Fold rate	Drift	Fold direction	Comments
3000	~	0.25	None	Backwards	
2400	~	1.50	None	Backwards	
1800	¤	0.25	None	Backwards	Only fold is an unfolding
1300	~	0.25	None	Backwards	
900	~	0	None	None	
600	~	0	Backwards	None	

Table 16: 130607-RecA-T4-wide-5. T4 DNA. Started at 3000 nm channel. $L/l_P = 9.89$

D	Initial condition	Fold rate	Drift	Fold direction
3000	~	0	None	None
2400	~	0	None	None
1800	~	0	None	None
1300	~	0	None	None
900	~	0	None	None
600	~	0	Forwards	None

Table 17: 130607-RecA-T4-wide-6. T4 DNA. Started at 3000 nm channel. $L/l_P = 7.84$

D	Initial condition	Fold rate	Drift	Fold direction
3000	~	0	None	None
2400	~	0	None	None
1800	~	0	None	None
1300	~	0	Forwards	None
900	~	0	None	None
600	~	0	None	None

Table 18: 130905-RecA-T4-narrow-1. T4 DNA. Started at 600 nm channel. $L/l_P = 14.97$

D	Initial condition	Fold rate	Drift	Fold direction
600	~	0	Both	None
900	~	0	None	None
1300	~	0	Forwards	None

Table 19: 130905-RecA-T4-narrow-2. T4 DNA. Started at 600 nm channel. $L/l_P = 12.82$

D	Initial condition	Fold rate	Drift	Fold direction
600	~	0	Forwards	None
900	~	0	None	None
1300	~	0	None	None
1800	~	0	Forwards	None
2400	~	0	None	None

Table 20: 130905-RecA-T4-narrow-3. T4 DNA. Started at 600 nm channel. $L/l_P = 13.75$

D	Initial condition	Fold rate	Drift	Fold direction	Comments
600	~	0	Both	None	
900	~	0	None	None	
1300	~	0	Both	None	
1800	¤	0	None	Backwards	Remains in initial condition throughout

Table 21: 130905-RecA-T4-narrow-4. T4 DNA. Started at 600 nm channel. $L/l_P = 18.68$

D	Initial condition	Fold rate	Drift	Fold direction	Comments
600	~	0	None	None	
900	~	0	None	None	
1300	~	0	None	None	
1800	σ, σ	0	Backwards	Both	Remains σ, σ throughout. Brighter region near rightmost loop suggests stuck to itself.

Table 22: 130905-RecA-T4-narrow-5. T4 DNA. Started at 600 nm channel. $L/l_P = 16.17$

D	Initial condition	Fold rate	Drift	Fold direction
600	~	0	None	None
900	~	0	None	None
1300	~	0	None	None
1800	~	0	Both	None

Table 23: 130905-RecA-T4-narrow-6. T4 DNA. Started at 600 nm channel. $L/l_P = 11.96$

D	Initial condition	Fold rate	Drift	Fold direction
1300	~	0	None	None
1800	~	0	None	None
2400	~	0	Forwards	None
3000	~	0.50	None	Backwards

Table 24: 130905-RecA-T4-narrow-7. T4 DNA. Started at 600 nm channel. $L/l_P = 13.28$

D	Initial condition	Fold rate	Drift	Fold direction
2400	▷	0.75	None	Backwards
3000	∞	0	Both	Forwards

Table 25: 130905-RecA-T4-wide-1. T4 DNA. Started at 3000 nm channel. $L/l_P = 10.43$

D	Initial condition	Fold rate	Drift	Fold direction
3000	~	1.50	Forwards	Forwards

Table 26: 130905-RecA-T4-wide-2. T4 DNA. Started at 3000 nm channel. $L/l_P = 11.36$

D	Initial condition	Fold rate	Drift	Fold direction	Comments
3000	~	0.75	Forwards	Neither	Bright clump on right end
2400	~	0	Both	None	Bright clump on right end
1800	~	0	Forwards	None	Bright clump on right end
1300	~	0	None	None	Bright clump on right end

Table 27: 130905-RecA-T4-wide-3. T4 DNA. Started at 3000 nm channel. $L/l_P = 10.78$

D	Initial condition	Fold rate	Drift	Fold direction	Comments
3000	~	1.00	None	Backwards	
2400	~	0	None	None	
1800	~	0	None	None	
1300	~	0	None	None	
900	σ (tight loop)	0	Forwards	Backwards	Bend suggestive of experimental error,

600	σ (tight loop)	0	Both	Backwards	but at wrong end.. Bend seemingly residual of that introduced at 900 nm.
-----	-----------------------	---	------	-----------	--

Table 28: 130905-RecA-T4-wide-4. T4 DNA. Started at 3000 nm channel. $L/l_P = 17.90$

D	Initial condition	Fold rate	Drift	Fold direction
3000	~	0	None	None
2400	~	0	None	None
1800	~	0	None	None
1300	~	0	None	None

Table 29: 130905-RecA-T4-wide-5. T4 DNA. Started at 3000 nm channel. $L/l_P = 15.54$

D	Initial condition	Fold rate	Drift	Fold direction
3000	~	0	None	None
1800	~	0	None	None

Table 30: 130905-RecA-T4-wide-6. T4 DNA. Started at 3000 nm channel. $L/l_P = 14.79$

D	Initial condition	Fold rate	Drift	Fold direction
3000	Ω (longer tails)	0.50	None	Forwards
2400	~	0	None	None
1800	~	0	None	None
1300	~	0	None	None
900	~	0	None	None

Table 31: 130905-RecA-T4-wide-7. T4 DNA. Started at 3000 nm channel. $L/l_P = 12.85$

D	Initial condition	Fold rate	Drift	Fold direction	Comments
3000	~	1.00	Forwards	Forwards	
2400	~	0	None	None	
1800	~	0	Backwards	None	
1300	~	0	None	None	
900	~	0	None	None	
600	σ	0	None	Backwards	Remains in initial condition throughout. Initial condition suggestive of experimental error, but at wrong end..

Table 32: 130905-RecA-T4-wide-8. T4 DNA. Started at 3000 nm channel. $L/l_P = 18.36$

D	Initial condition	Fold rate	Drift	Fold direction	Comments
3000	~	0	None	None	
2400	~	0.50	None	None	Filament seems to have a point around which bending is easier.
1800	σ	0	None	Backwards	See previous comment. This point is the origin of the σ bend.
1300	σ	0	None	Backwards	See previous comment.

Table 33: 130924-RecA-lambda-narrow-1. λ DNA. Started at 600 nm channel. $L/l_P = 9.98$

D	Initial condition	Fold rate	Drift	Fold direction
---	-------------------	-----------	-------	----------------

600	~	0	Both	None
900	~	0	Both	None
1300	~	0	Both	None
1800	~	0	Forwards	None
2400	~	0	Both	None
3000	~	0	None	None

Table 34: 130924-RecA-lambda-narrow-2. λ DNA. Started at 600 nm channel. $L/l_p = 17.65$

D	Initial condition	Fold rate	Drift	Fold direction
600	~	0	Both	None
1300	~	0	None	None

Table 35: 130924-RecA-lambda-narrow-3. λ DNA. Started at 600 nm channel. $L/l_p = 14.92$

D	Initial condition	Fold rate	Drift	Fold direction
600	~	0	Both	None
900	~	0	Both	None

Table 36: 130924-RecA-lambda-narrow-4. λ DNA. Started at 600 nm channel. $L/l_p = 17.30$

D	Initial condition	Fold rate	Drift	Fold direction
600	~	0	None	None

Table 37: 130924-RecA-lambda-narrow-5. λ DNA. Started at 600 nm channel. $L/l_p = 13.25$

D	Initial condition	Fold rate	Drift	Fold direction
600	~	0	Both	None
900	~	0	Both	None
1300	~	0	Both	None
1800	~	0	None	None
2400	~	0	None	None
3000	~	0.75	Both	Neither

Table 38: 130924-RecA-lambda-narrow-6. λ DNA. Started at 600 nm channel. $L/l_p = 14.40$

D	Initial condition	Fold rate	Drift	Fold direction
600	~	0	Both	None
900	~	0	Both	None
1300	~	0	Forwards	None

Table 39: 130924-RecA-lambda-wide-1. λ DNA. Started at 3000 nm channel. $L/l_p = 13.88$

D	Initial condition	Fold rate	Drift	Fold direction
3000	~	0	Forwards	None
2400	~	0	Both	None

Table 40: 130924-RecA-lambda-wide-10. λ DNA. Started at 3000 nm channel. $L/l_p = 12.37$

D	Initial condition	Fold rate	Drift	Fold direction
3000	~	0.75	Forwards	Neither

2400	\sim	0.25	Backwards	Neither
------	--------	------	-----------	---------

Table 41: 130924-RecA-lambda-wide-2. λ DNA. Started at 3000 nm channel. $L/l_p = 20.29$

D	Initial condition	Fold rate	Drift	Fold direction
3000	\sim	0.50	None	Forwards
2400	\sim	0	None	None

Table 42: 130924-RecA-lambda-wide-3. λ DNA. Started at 3000 nm channel. $L/l_p = 14.42$

D	Initial condition	Fold rate	Drift	Fold direction	Comments
3000	\sim	0.50	Backwards	Forwards	
2400	\bowtie	0	None	Forwards	Suggests experimental error

Table 43: 130924-RecA-lambda-wide-4. λ DNA. Started at 3000 nm channel. $L/l_p = 13.82$

D	Initial condition	Fold rate	Drift	Fold direction	Comments
3000	\sim	1.50	None	Neither	Suspicious bend like \bowtie (with bright spot)
2400	\sim	0.25	Backwards	Neither	See previous comment
1300	\sim	0	Forwards	None	

Table 44: 130924-RecA-lambda-wide-5. λ DNA. Started at 3000 nm channel. $L/l_p = 11.72$

D	Initial condition	Fold rate	Drift	Fold direction
3000	\subset	1.00	None	Neither
2400	\sim	0	None	None
1300	\sim	0	Both	None
900	\sim	0	None	None
600	\sim	0	Both	None

Table 45: 130924-RecA-lambda-wide-8. λ DNA. Started at 3000 nm channel. $L/l_p = 14.74$

D	Initial condition	Fold rate	Drift	Fold direction	Comments
3000	\sim	1.25	None	Neither	
2400	\sim	0	None	None	Sometimes seems to want to form \bowtie
1800	\sim	0.25	None	Neither	See previous comment; this is the cause of the folding here (one fold, one unfold).
1300	\sim	0	None	None	
900	\sim	0	Forwards	None	
600	\sim	0	Forwards	None	

Table 46: 130924-RecA-lambda-wide-9. λ DNA. Started at 3000 nm channel. $L/l_p = 11.08$

D	Initial condition	Fold rate	Drift	Fold direction
3000	\sim	0	None	None

4 Kymographs

These kymographs were produced by stacking the intensity profiles produced for each sequence of frames as described above.

4.1 130603-RecA-T4-wide-2

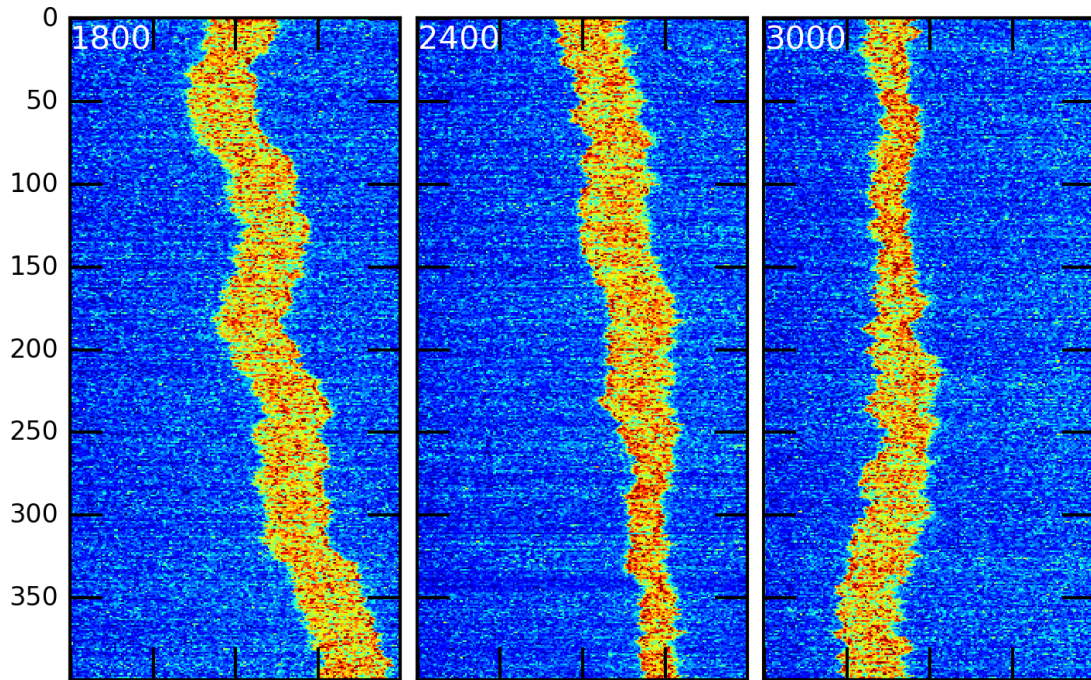


Figure 29: Vertical axis is time. White annotation gives channel width in nanometres.

4.2 130603-RecA-T4-wide-3

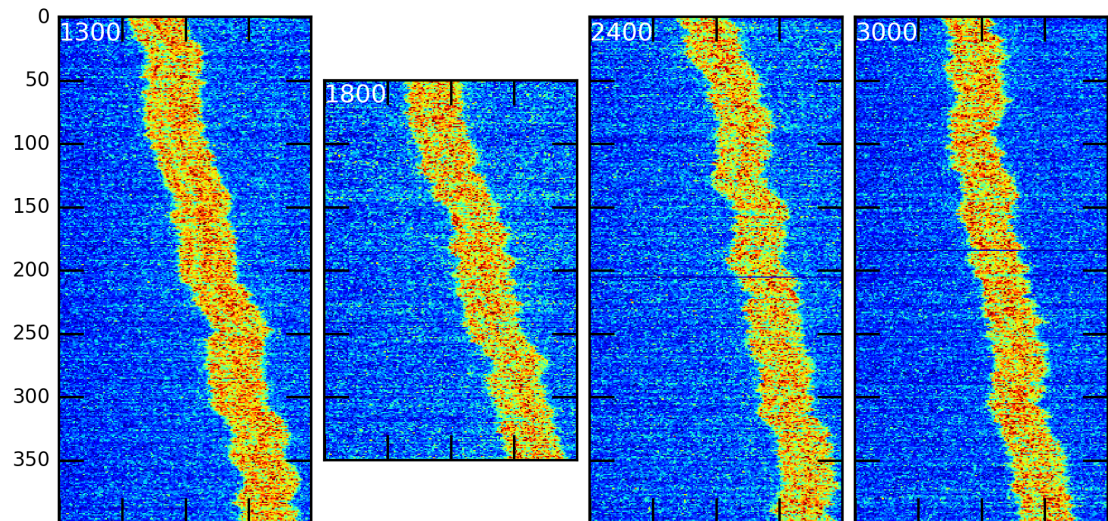


Figure 30: Vertical axis is time. White annotation gives channel width in nanometres.

4.3 130603-RecA-T4-wide-4

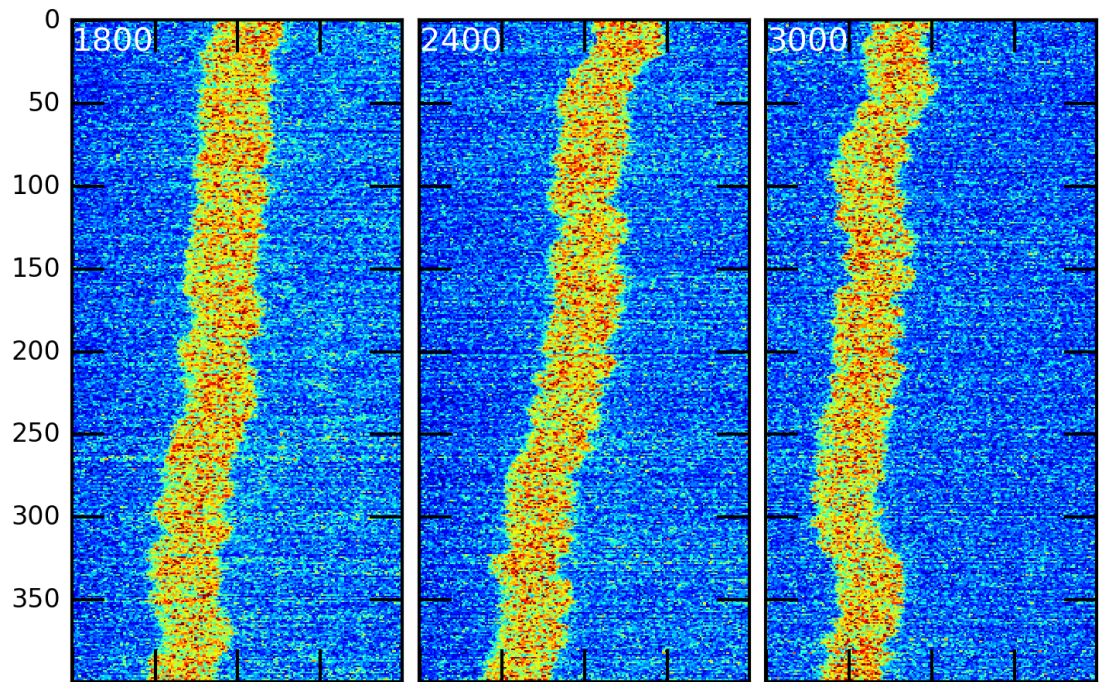


Figure 31: Vertical axis is time. White annotation gives channel width in nanometres.

4.4 130603-RecA-T4-wide-5

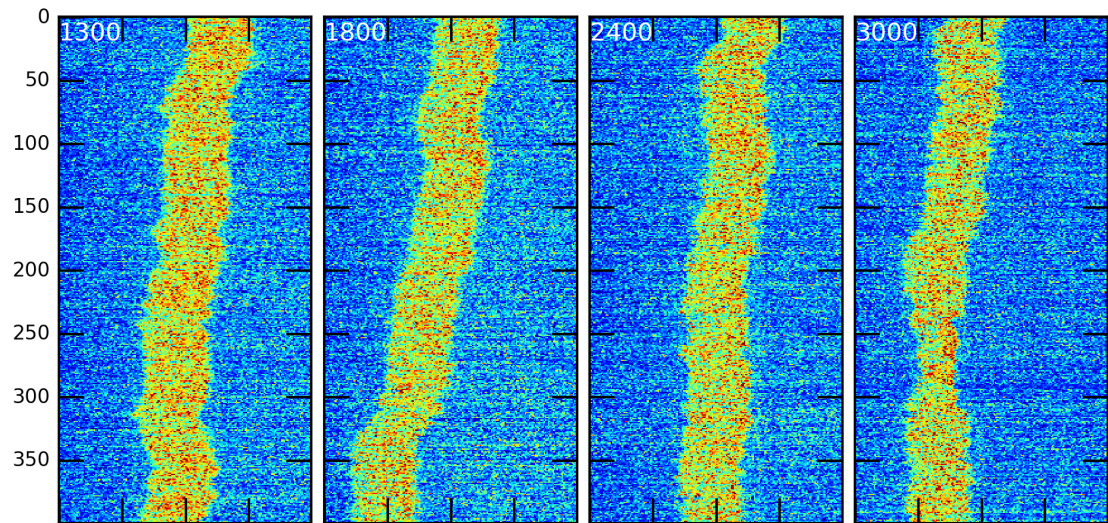


Figure 32: Vertical axis is time. White annotation gives channel width in nanometres.

4.5 130603-RecA-T4-wide-7

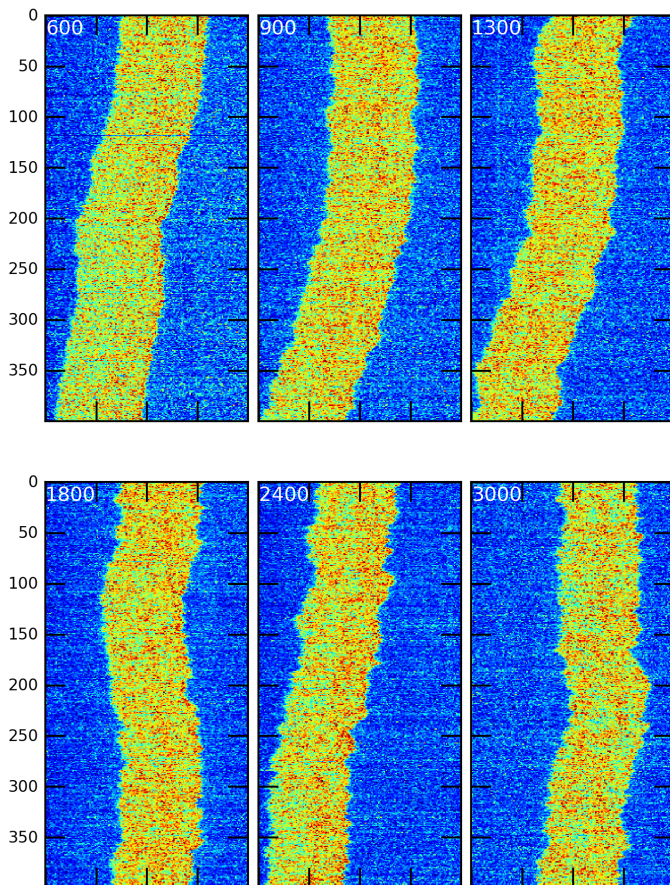


Figure 33: Vertical axis is time. White annotation gives channel width in nanometres.

4.6 130607-RecA-T4-narrow-10

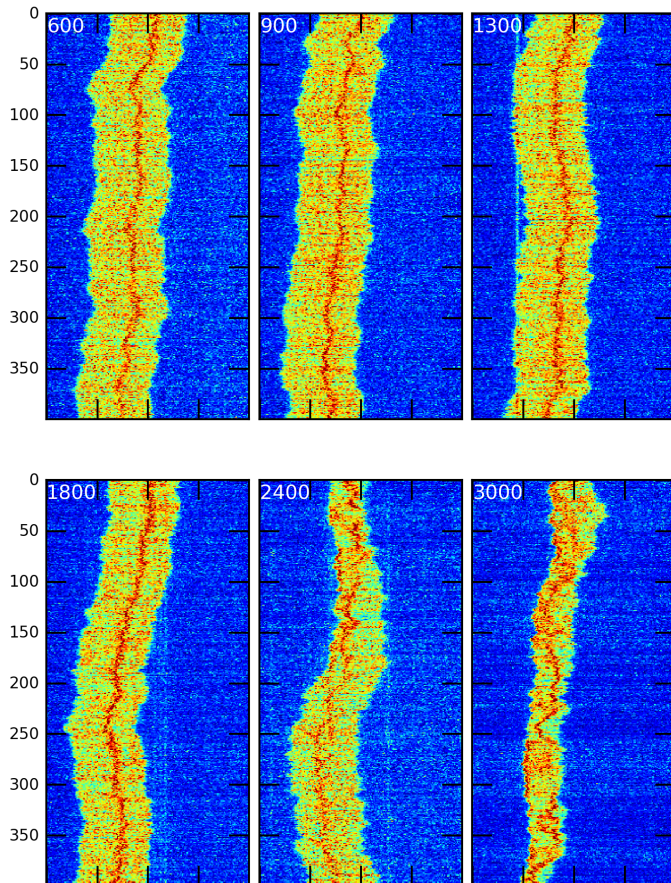


Figure 34: Vertical axis is time. White annotation gives channel width in nanometres.

4.7 130607-RecA-T4-narrow-7

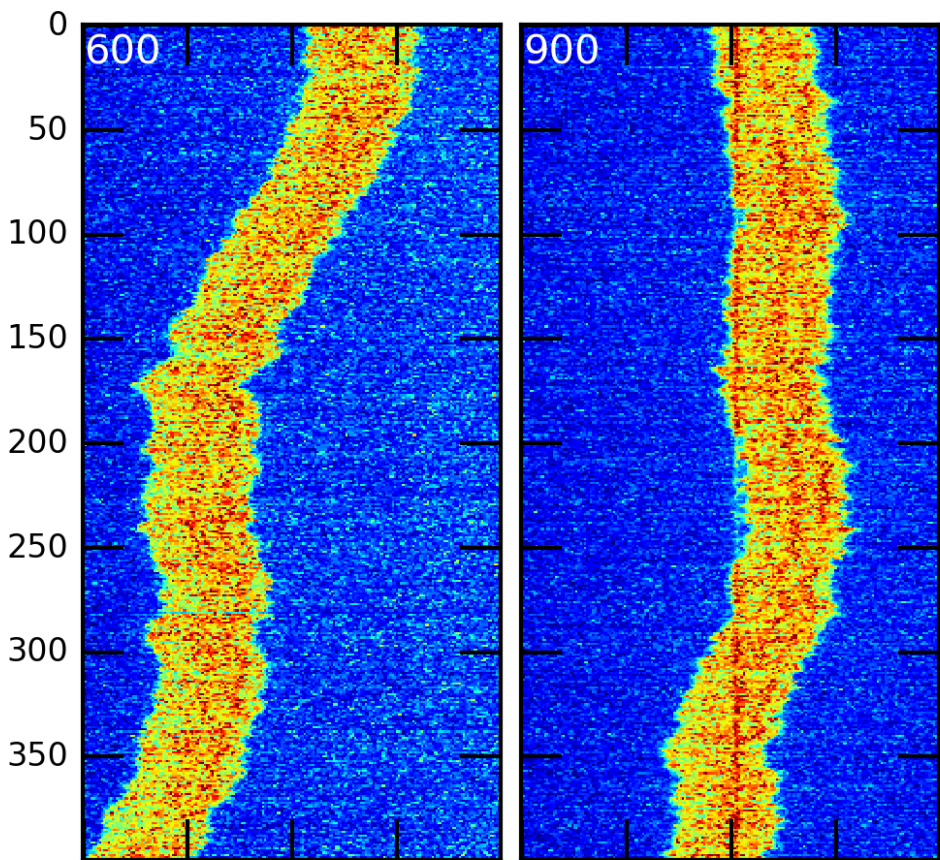


Figure 35: Vertical axis is time. White annotation gives channel width in nanometres.

4.8 130607-RecA-T4-narrow-8

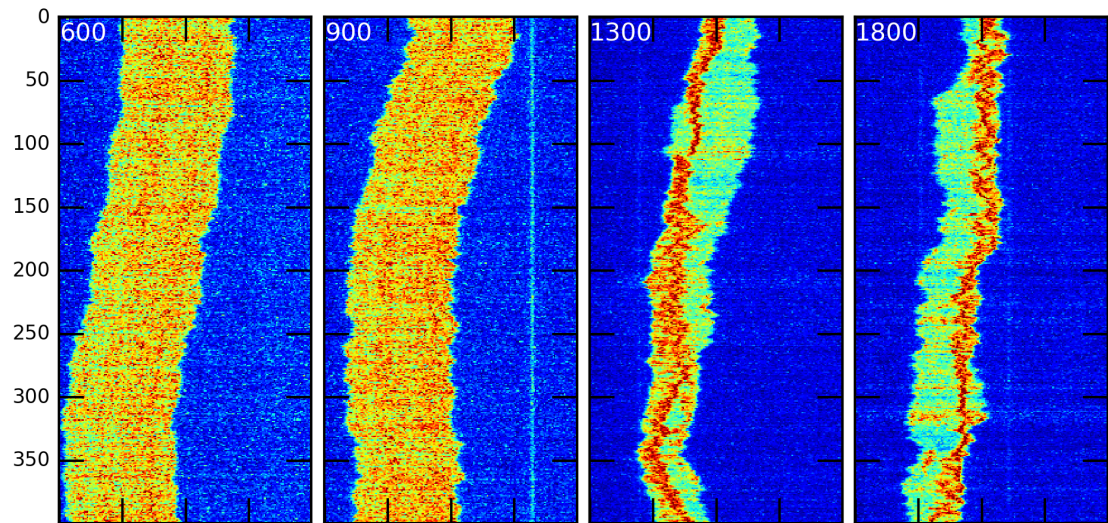


Figure 36: Vertical axis is time. White annotation gives channel width in nanometres.

4.9 130607-RecA-T4-narrow-9

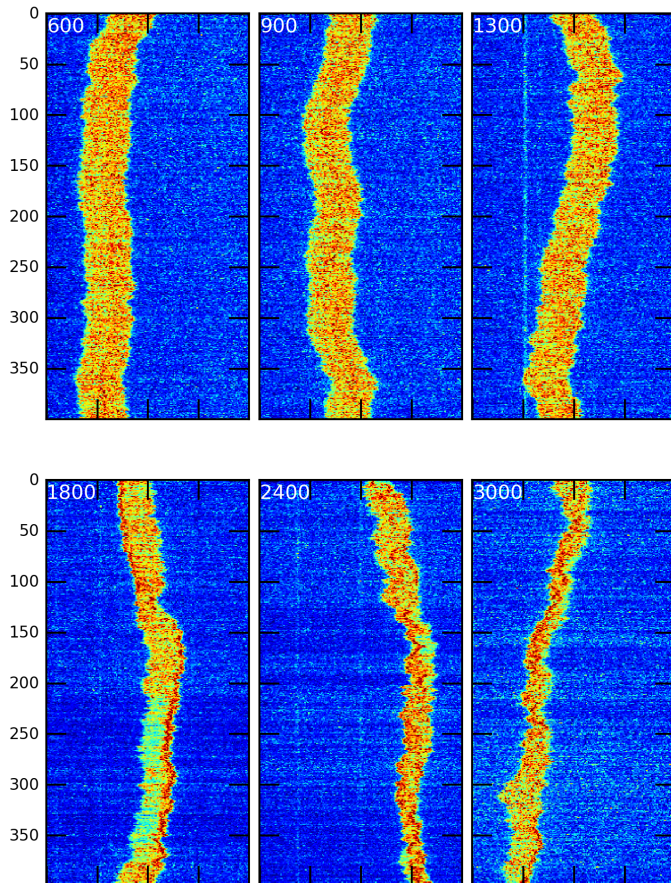


Figure 37: Vertical axis is time. White annotation gives channel width in nanometres.

4.10 130607-RecA-T4-wide-1

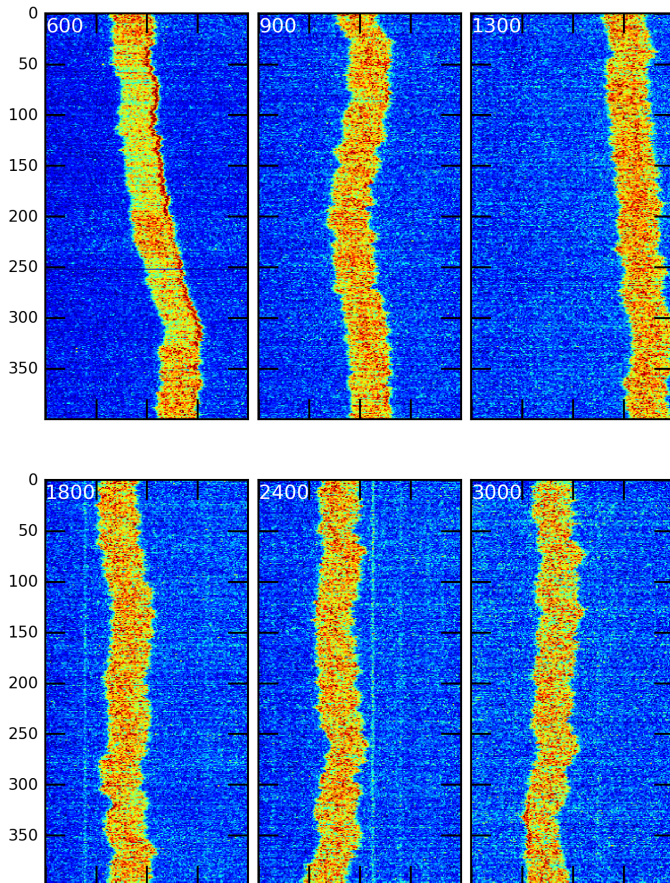


Figure 38: Vertical axis is time. White annotation gives channel width in nanometres.

4.11 130607-RecA-T4-wide-2

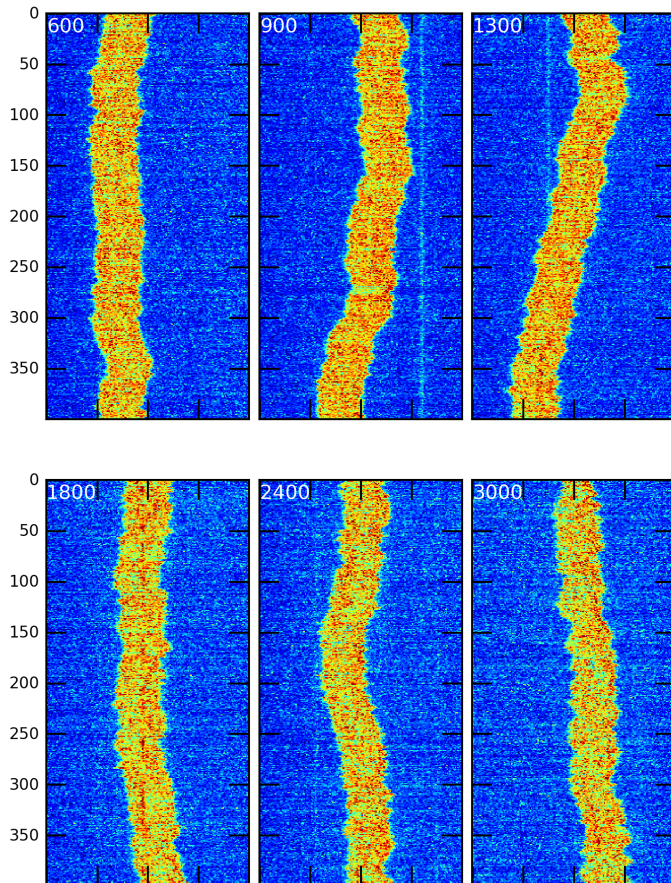


Figure 39: Vertical axis is time. White annotation gives channel width in nanometres.

4.12 130607-RecA-T4-wide-3

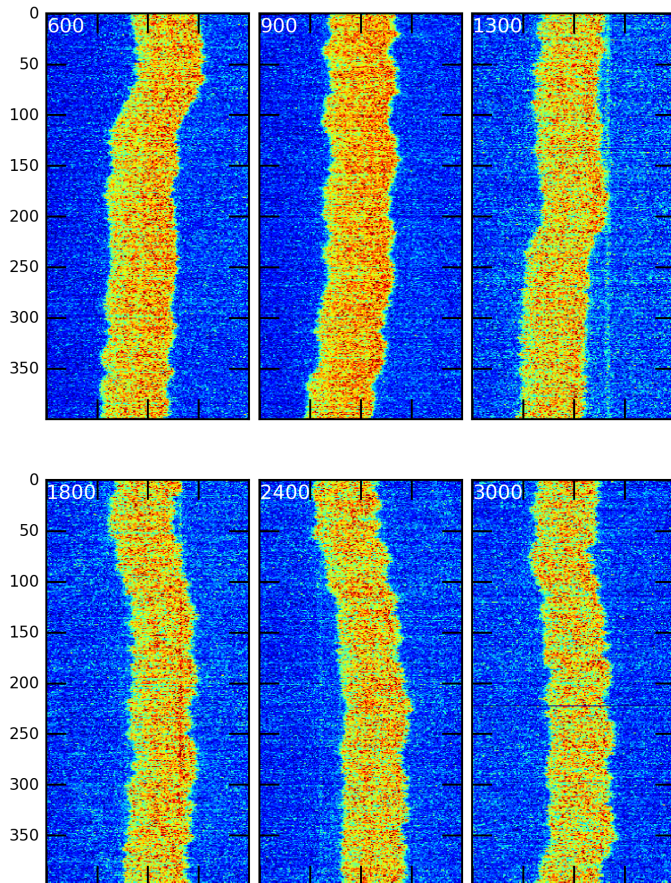


Figure 40: Vertical axis is time. White annotation gives channel width in nanometres.

4.13 130607-RecA-T4-wide-4

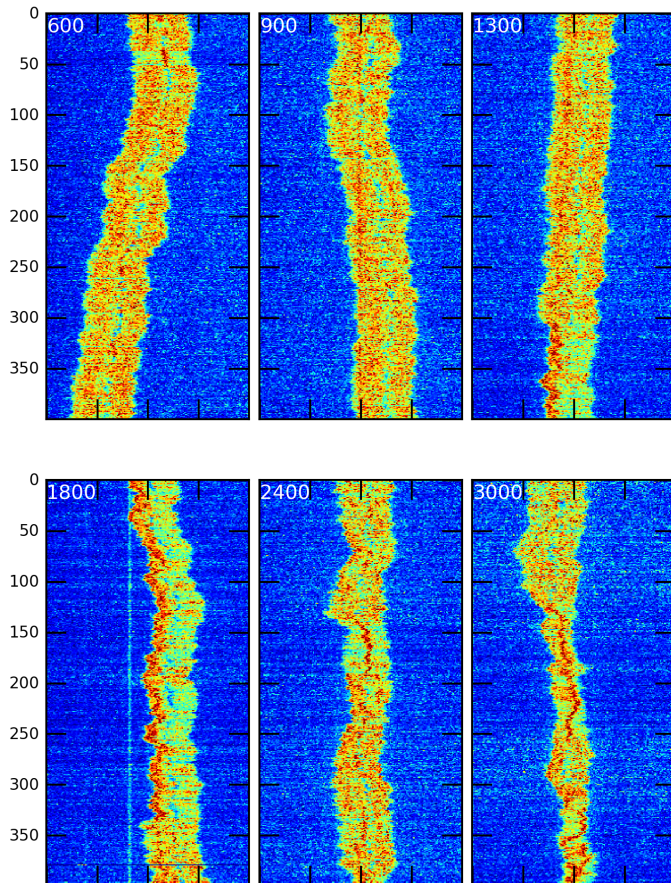


Figure 41: Vertical axis is time. White annotation gives channel width in nanometres.

4.14 130607-RecA-T4-wide-5

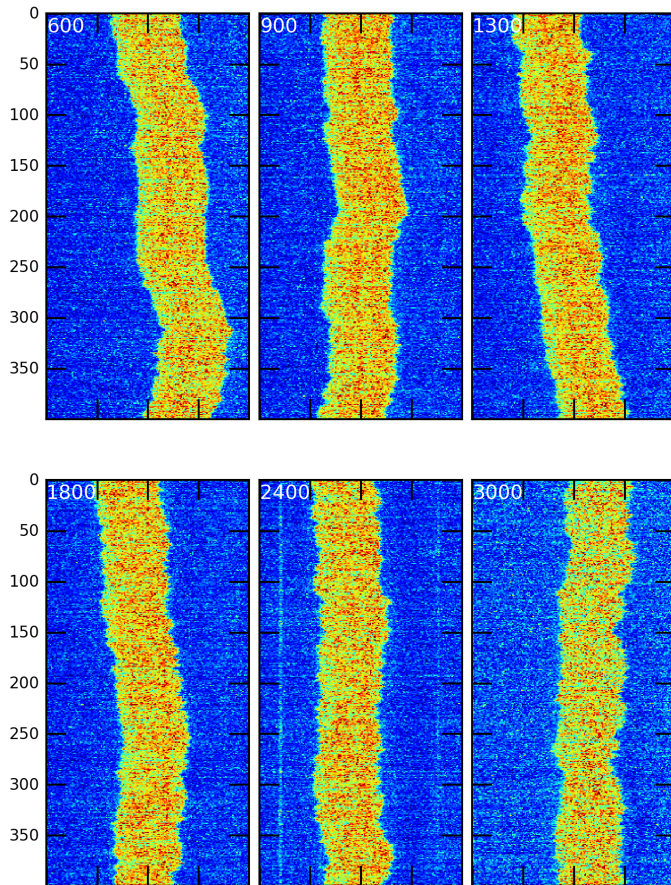


Figure 42: Vertical axis is time. White annotation gives channel width in nanometres.

4.15 130607-RecA-T4-wide-6

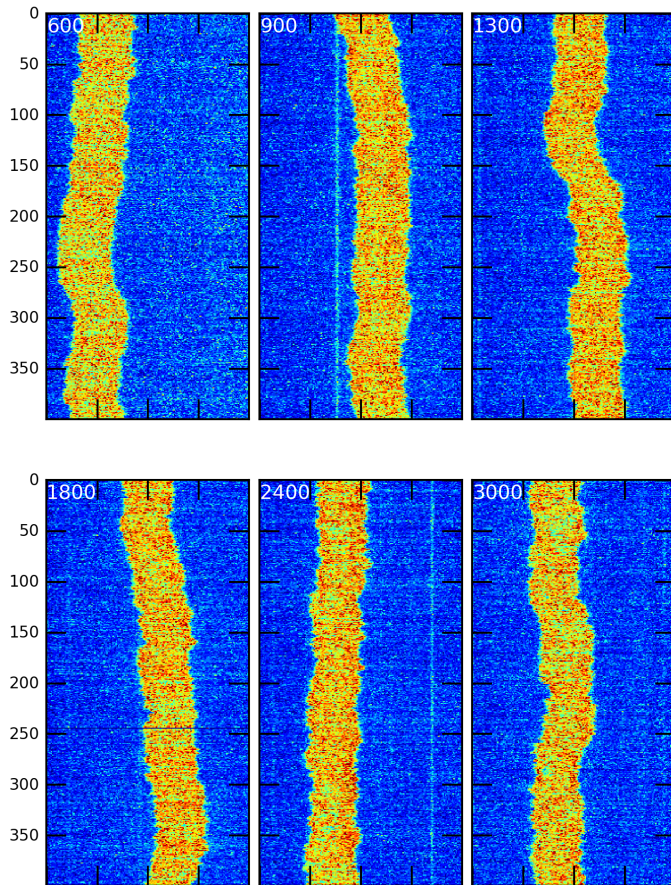


Figure 43: Vertical axis is time. White annotation gives channel width in nanometres.

4.16 130905-RecA-T4-narrow-1

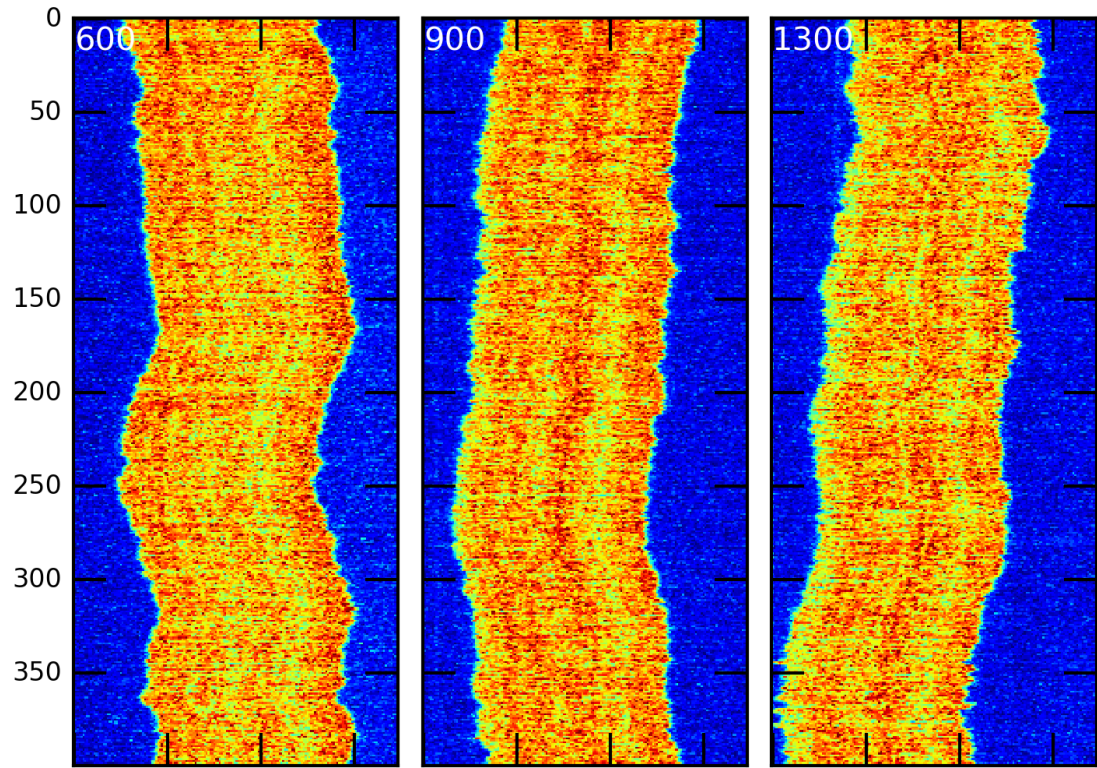


Figure 44: Vertical axis is time. White annotation gives channel width in nanometres.

4.17 130905-RecA-T4-narrow-2

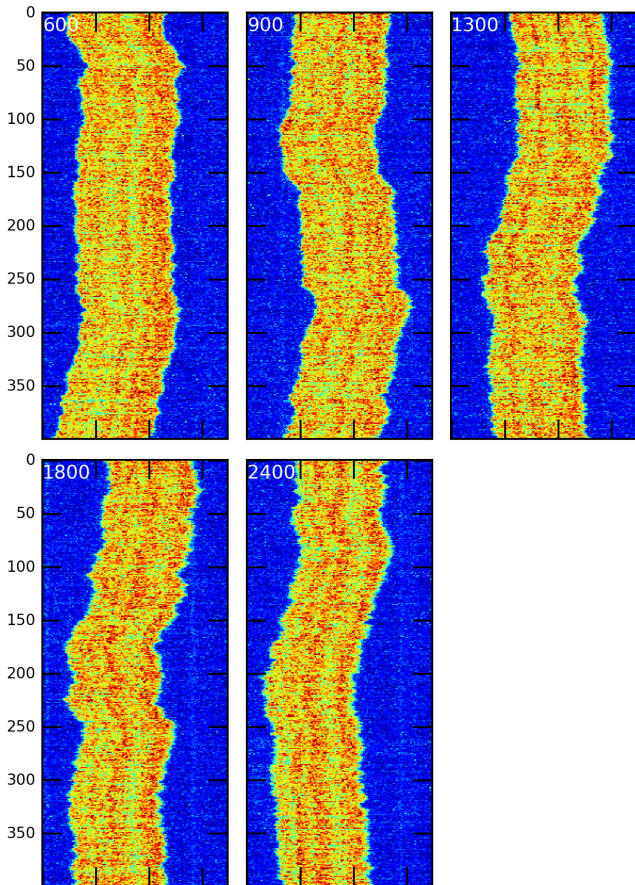


Figure 45: Vertical axis is time. White annotation gives channel width in nanometres.

4.18 130905-RecA-T4-narrow-3

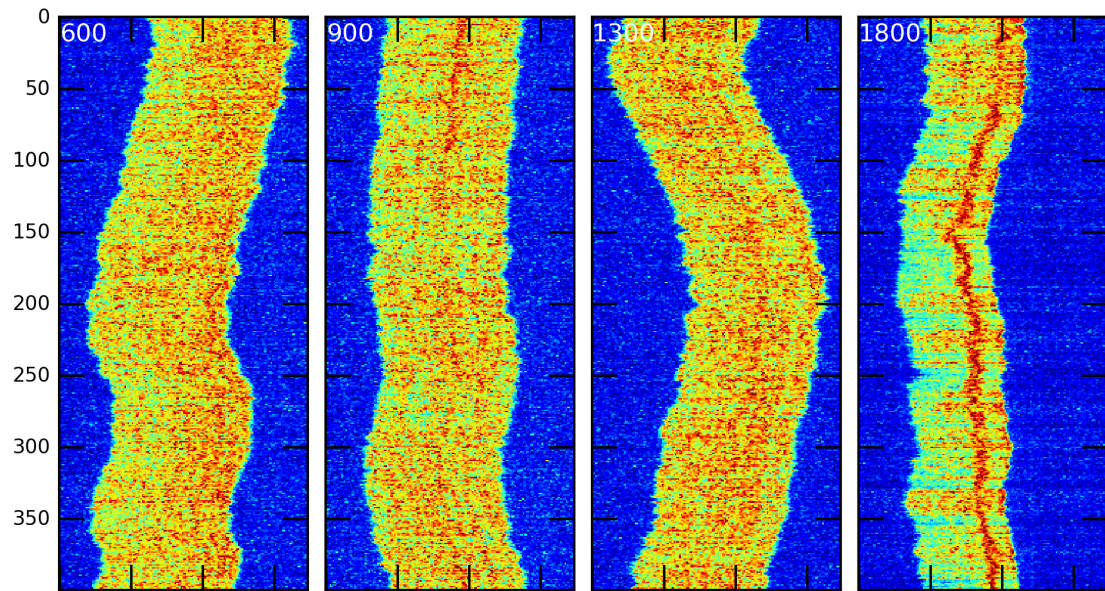


Figure 46: Vertical axis is time. White annotation gives channel width in nanometres.

4.19 130905-RecA-T4-narrow-4

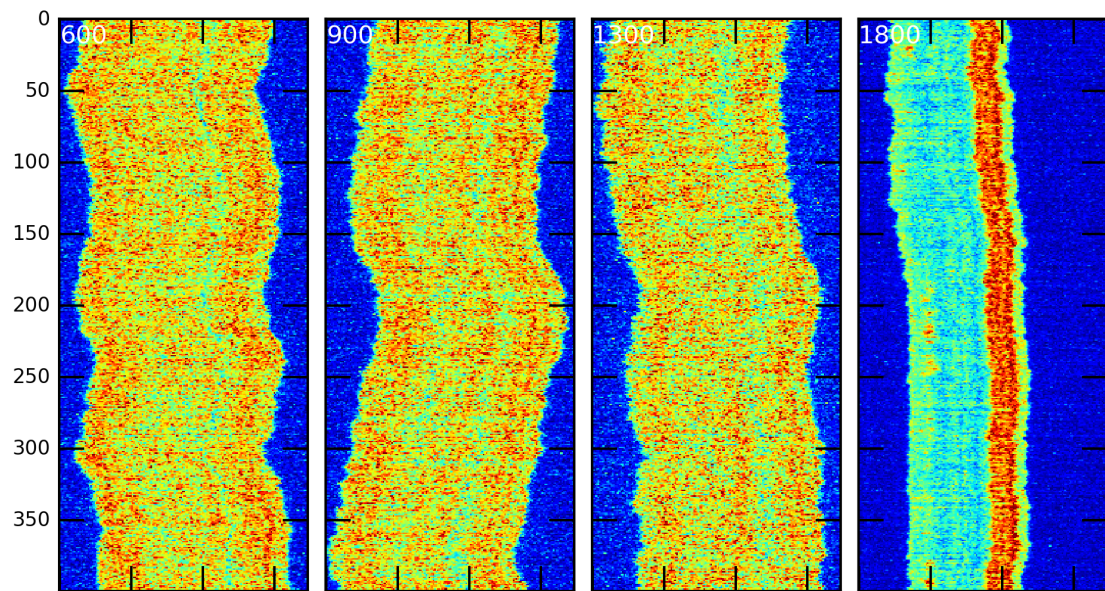


Figure 47: Vertical axis is time. White annotation gives channel width in nanometres.

4.20 130905-RecA-T4-narrow-5

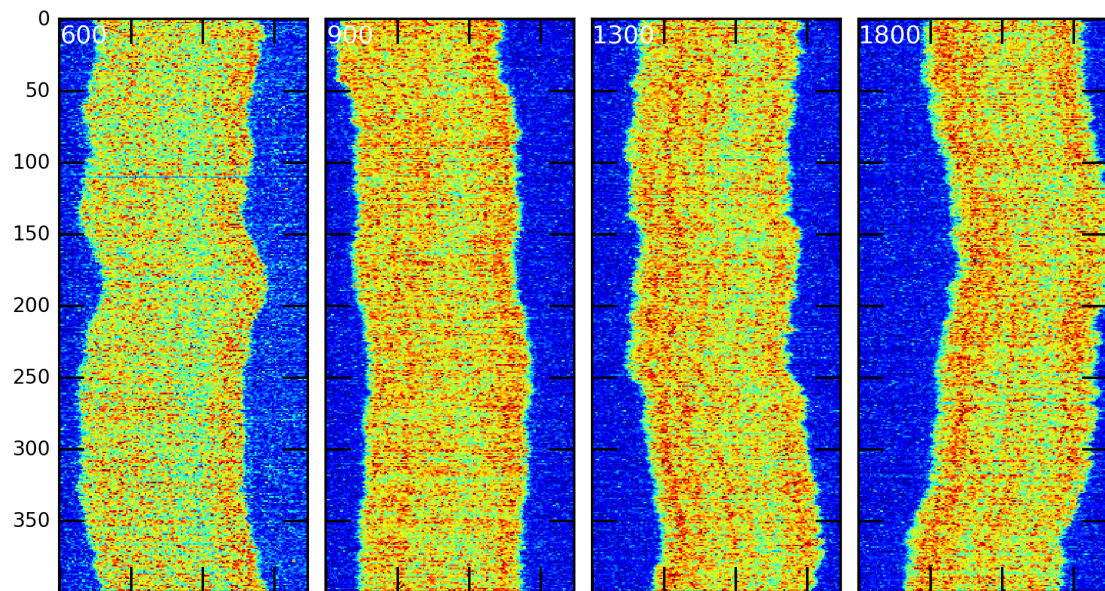


Figure 48: Vertical axis is time. White annotation gives channel width in nanometres.

4.21 130905-RecA-T4-narrow-6

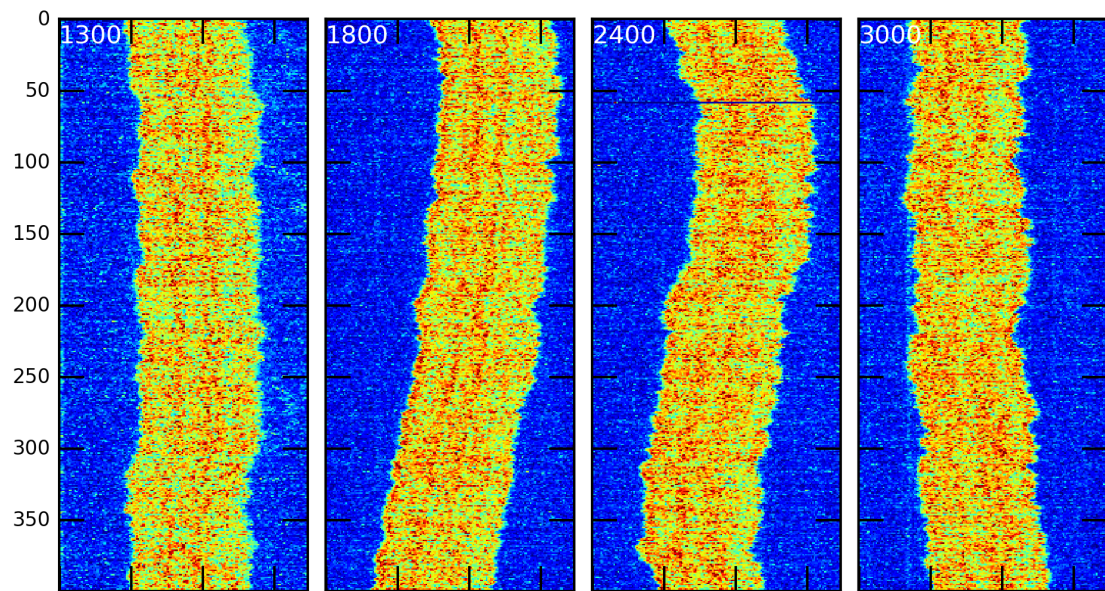


Figure 49: Vertical axis is time. White annotation gives channel width in nanometres.

4.22 130905-RecA-T4-narrow-7

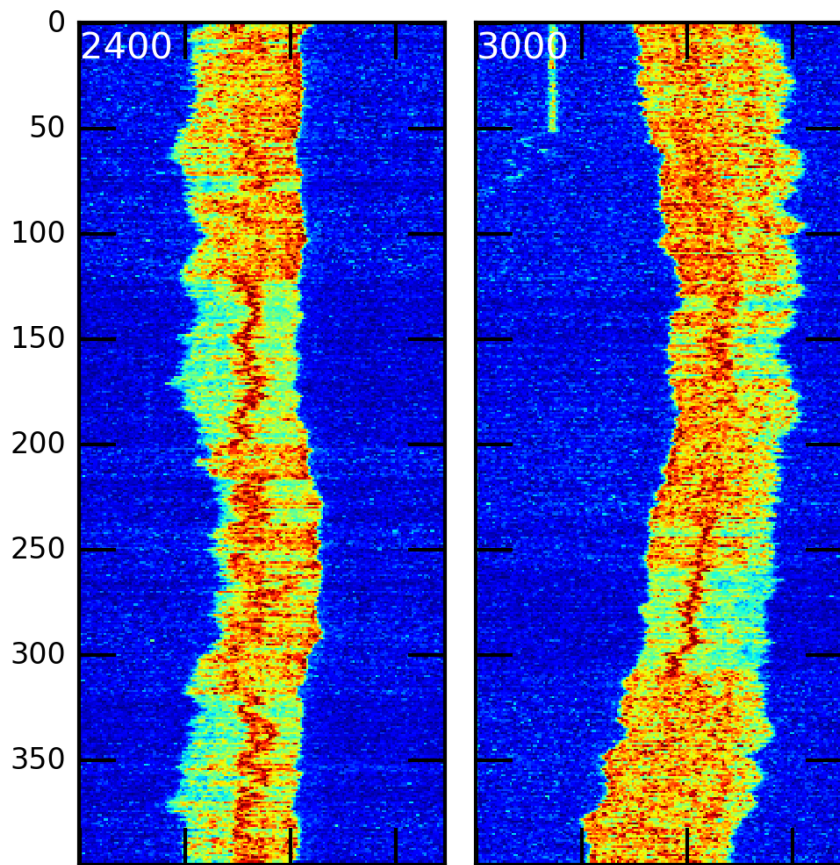


Figure 50: Vertical axis is time. White annotation gives channel width in nanometres.

4.23 130905-RecA-T4-wide-1

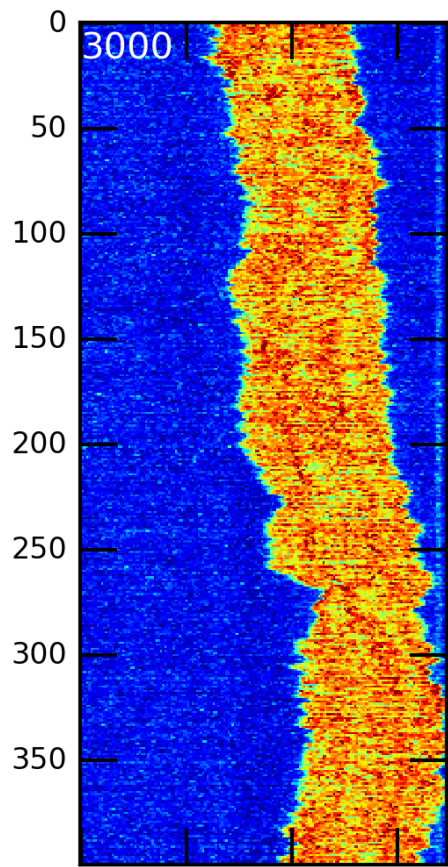


Figure 51: Vertical axis is time. White annotation gives channel width in nanometres.

4.24 130905-RecA-T4-wide-2

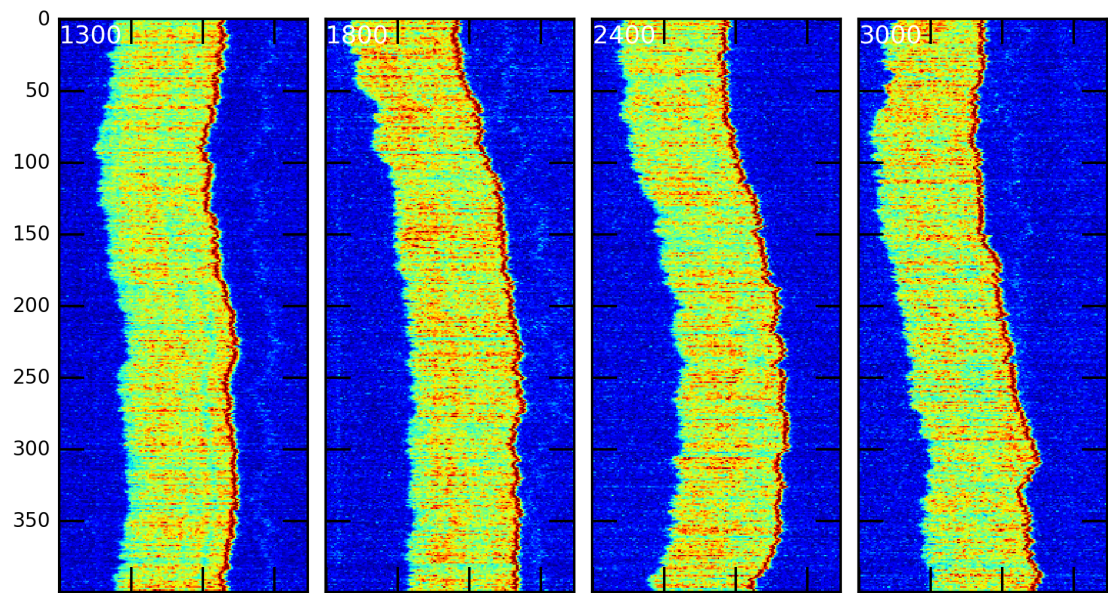


Figure 52: Vertical axis is time. White annotation gives channel width in nanometres.

4.25 130905-RecA-T4-wide-3

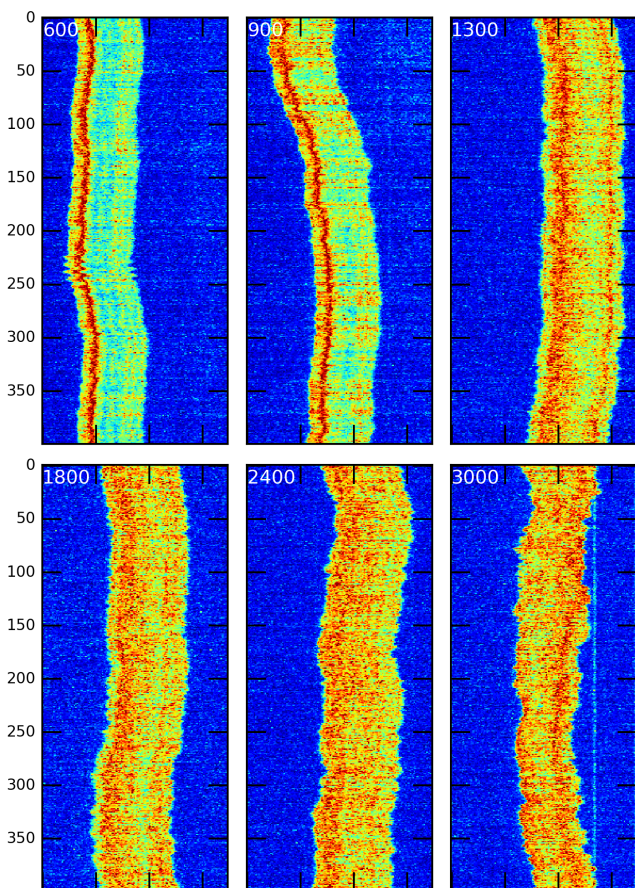


Figure 53: Vertical axis is time. White annotation gives channel width in nanometres.

4.26 130905-RecA-T4-wide-4

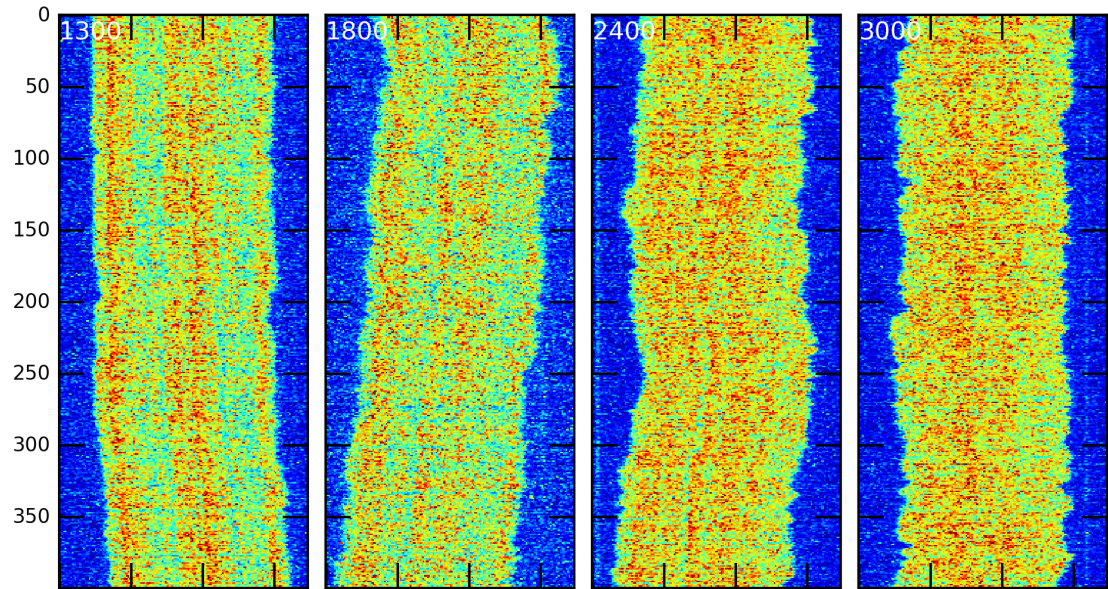


Figure 54: Vertical axis is time. White annotation gives channel width in nanometres.

4.27 130905-RecA-T4-wide-5

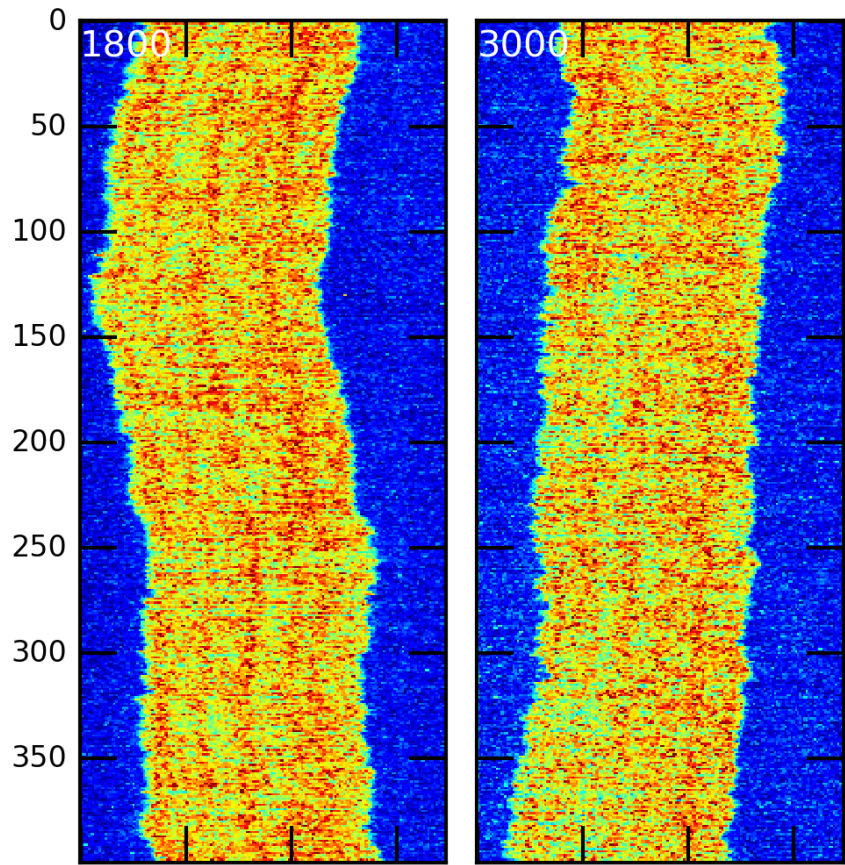


Figure 55: Vertical axis is time. White annotation gives channel width in nanometres.

4.28 130905-RecA-T4-wide-6

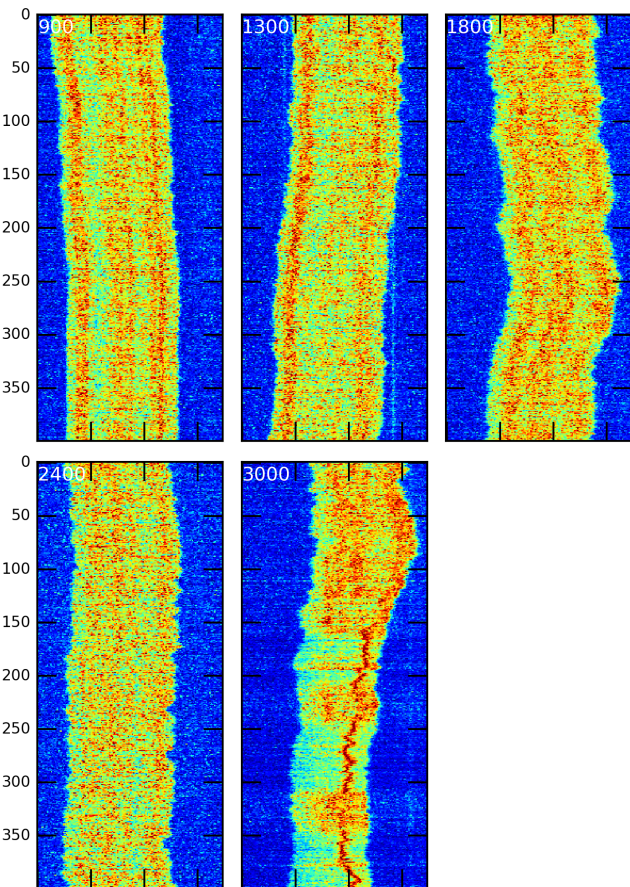


Figure 56: Vertical axis is time. White annotation gives channel width in nanometres.

4.29 130905-RecA-T4-wide-7

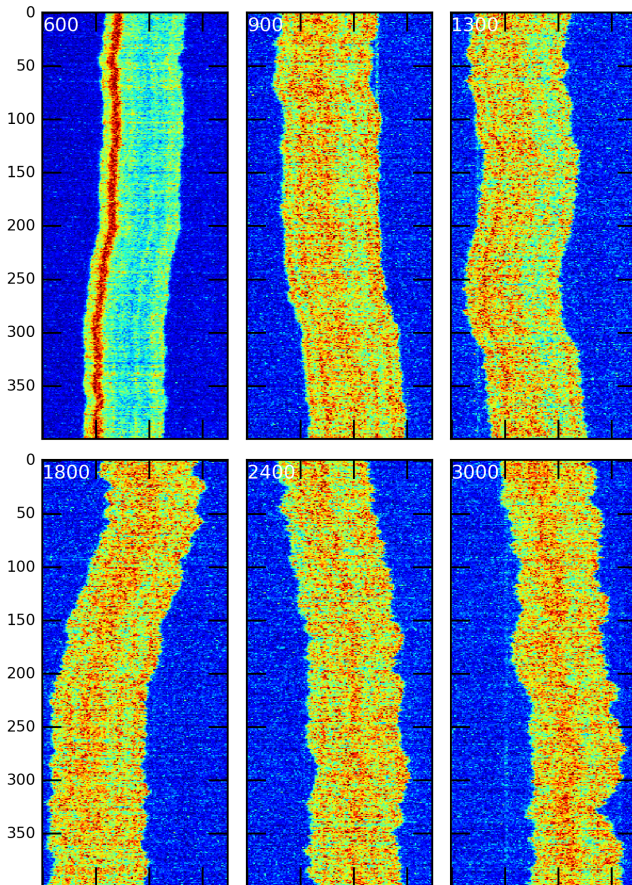


Figure 57: Vertical axis is time. White annotation gives channel width in nanometres.

4.30 130905-RecA-T4-wide-8

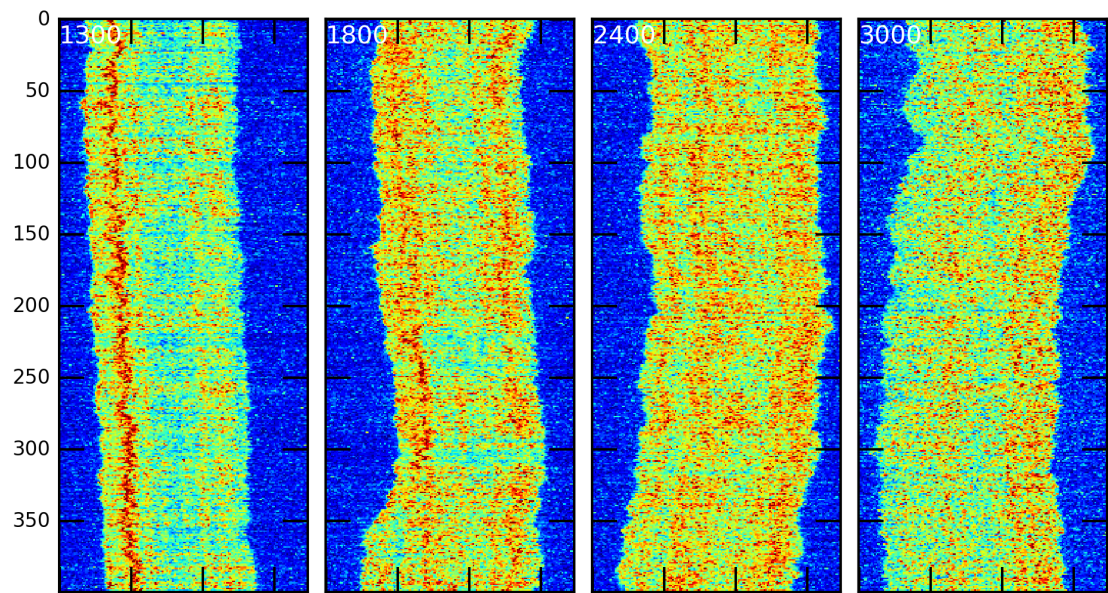


Figure 58: Vertical axis is time. White annotation gives channel width in nanometres.

4.31 130924-RecA-lambda-narrow-1

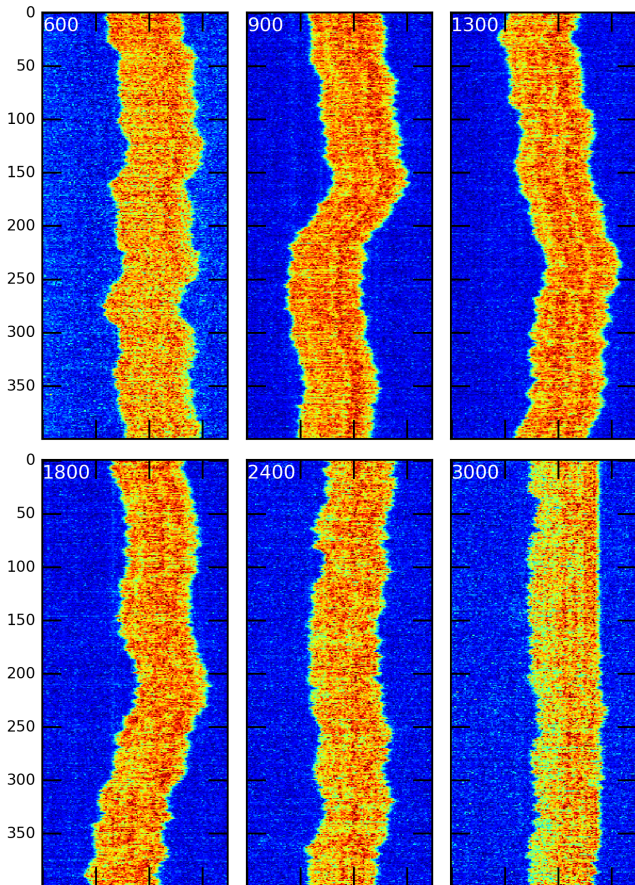


Figure 59: Vertical axis is time. White annotation gives channel width in nanometres.

4.32 130924-RecA-lambda-narrow-2

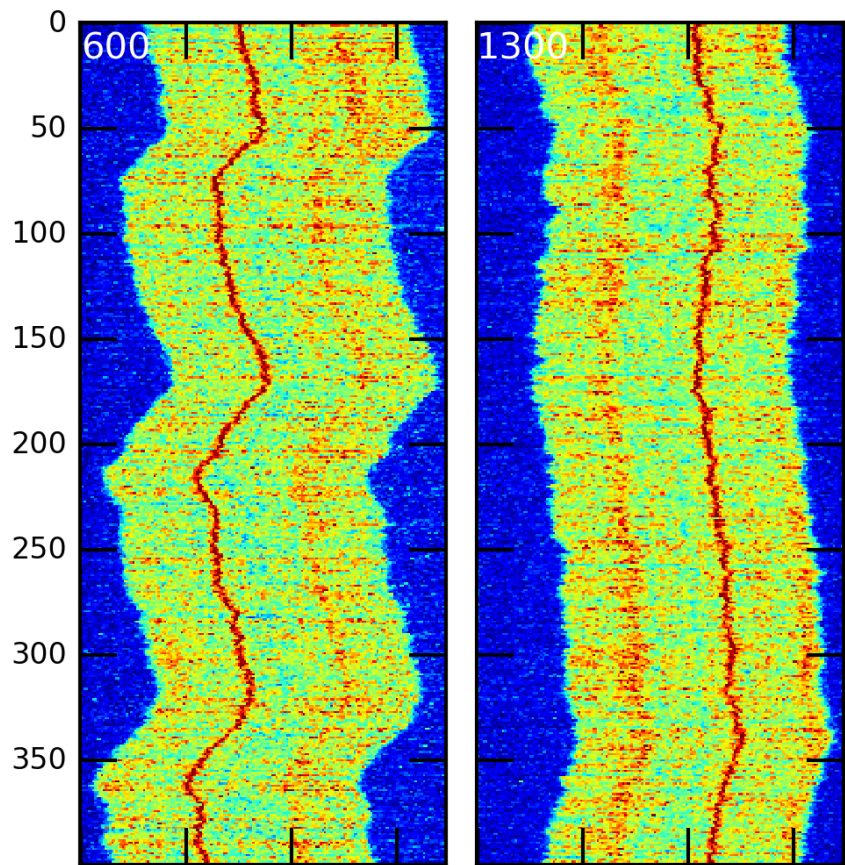


Figure 60: Vertical axis is time. White annotation gives channel width in nanometres.

4.33 130924-RecA-lambda-narrow-3

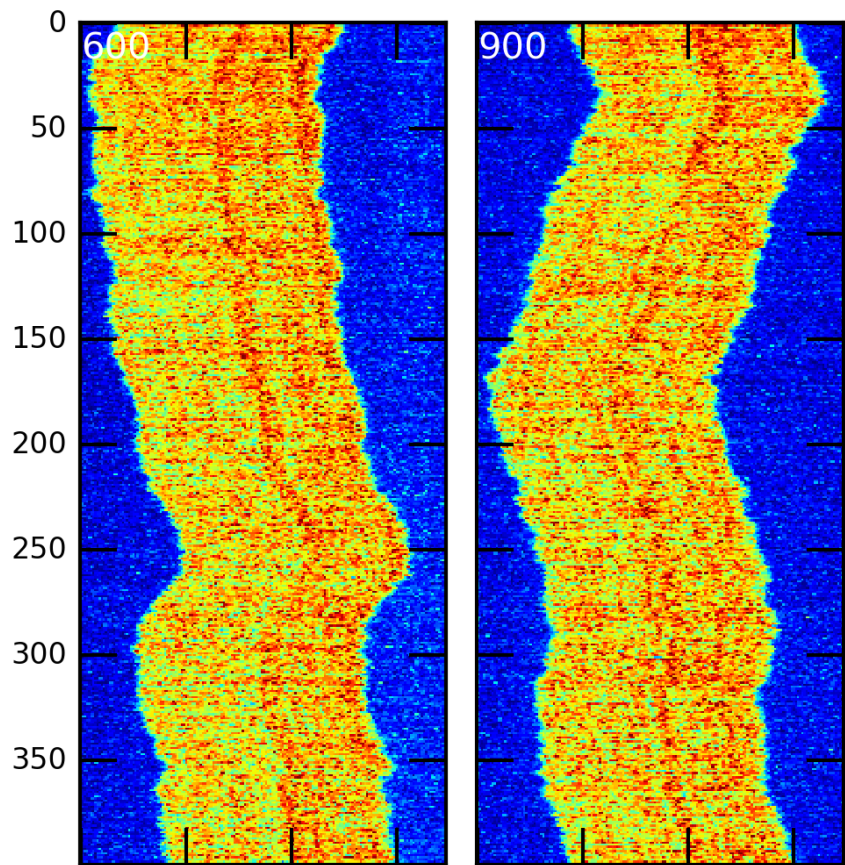


Figure 61: Vertical axis is time. White annotation gives channel width in nanometres.

4.34 130924-RecA-lambda-narrow-4

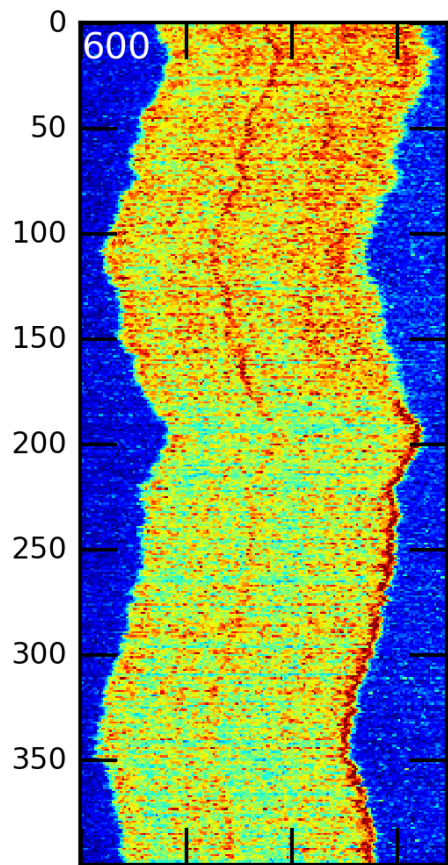


Figure 62: Vertical axis is time. White annotation gives channel width in nanometres.

4.35 130924-RecA-lambda-narrow-5

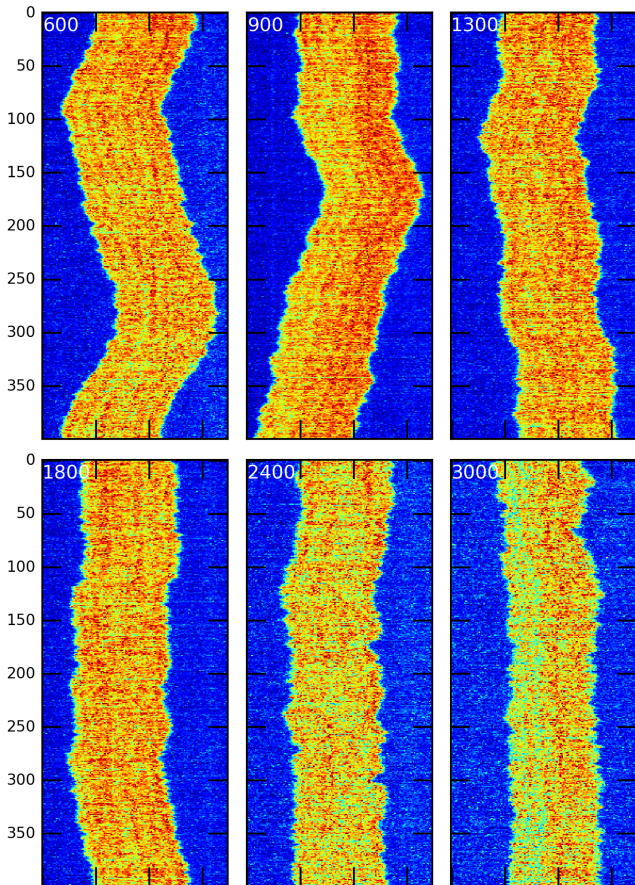


Figure 63: Vertical axis is time. White annotation gives channel width in nanometres.

4.36 130924-RecA-lambda-narrow-6

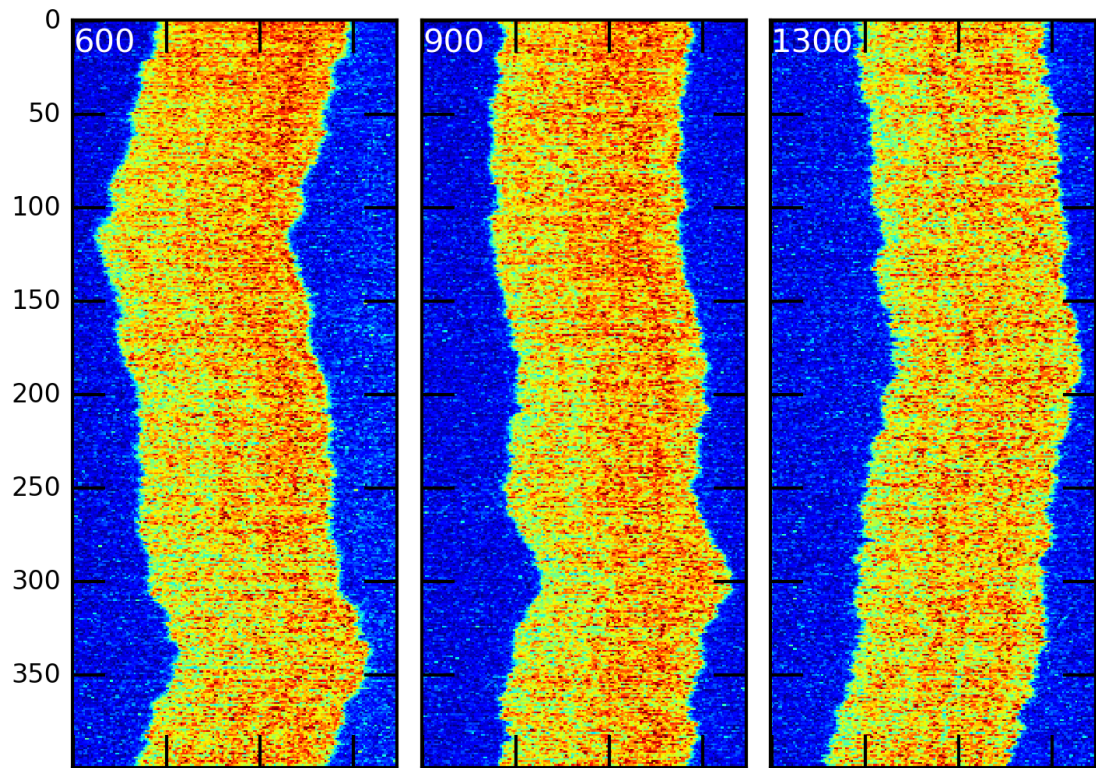


Figure 64: Vertical axis is time. White annotation gives channel width in nanometres.

4.37 130924-RecA-lambda-wide-1

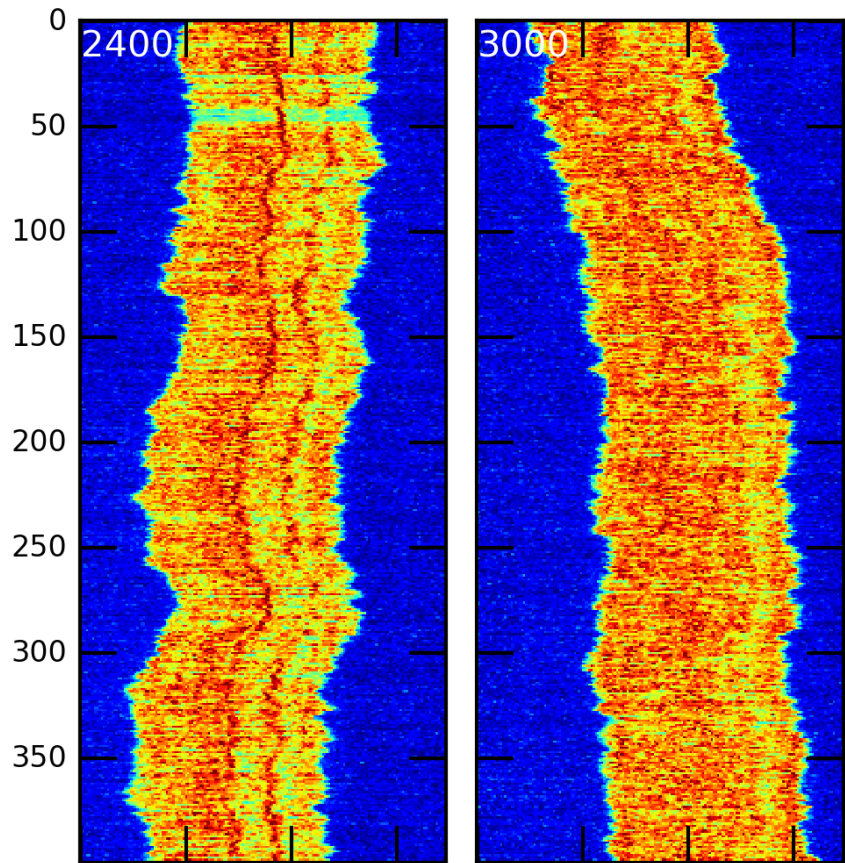


Figure 65: Vertical axis is time. White annotation gives channel width in nanometres.

4.38 130924-RecA-lambda-wide-10

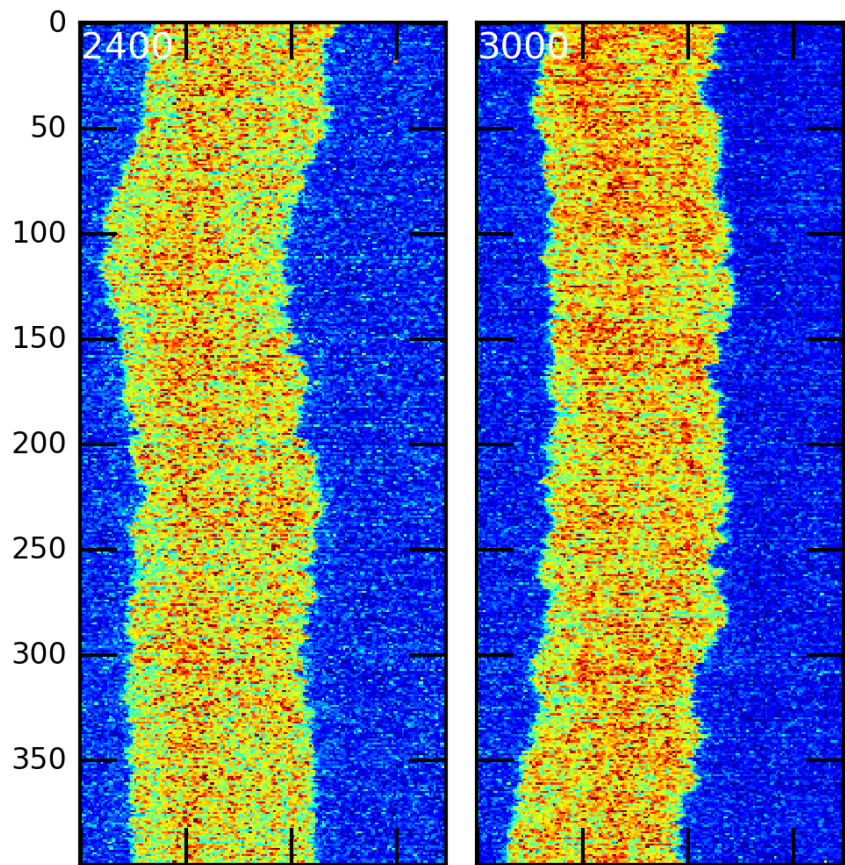


Figure 66: Vertical axis is time. White annotation gives channel width in nanometres.

4.39 130924-RecA-lambda-wide-2

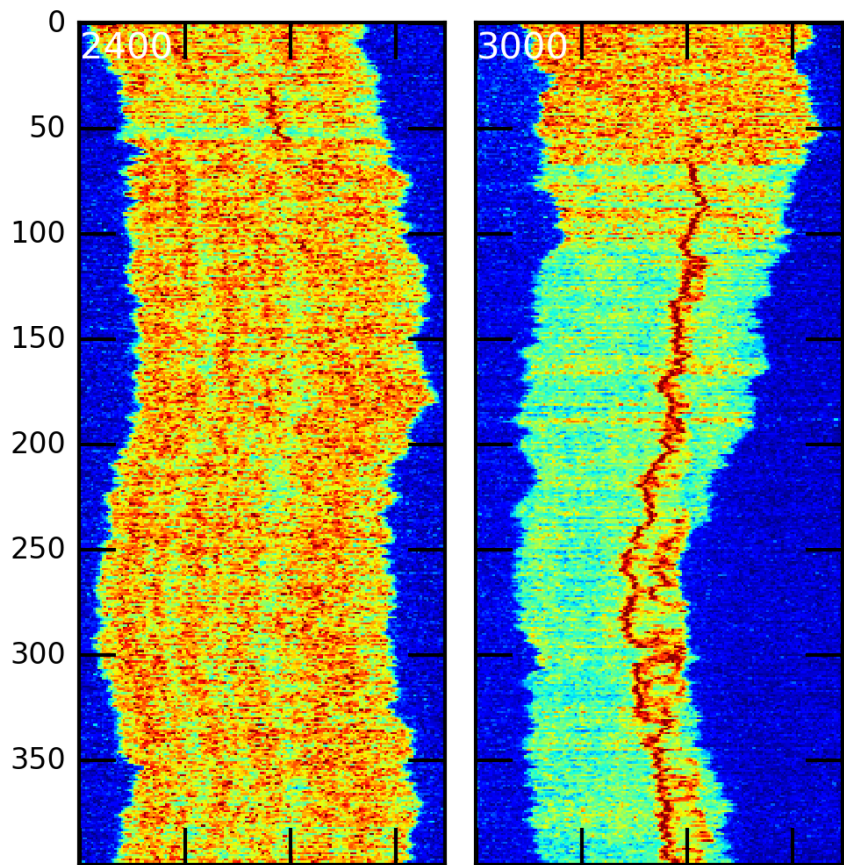


Figure 67: Vertical axis is time. White annotation gives channel width in nanometres.

4.40 130924-RecA-lambda-wide-3

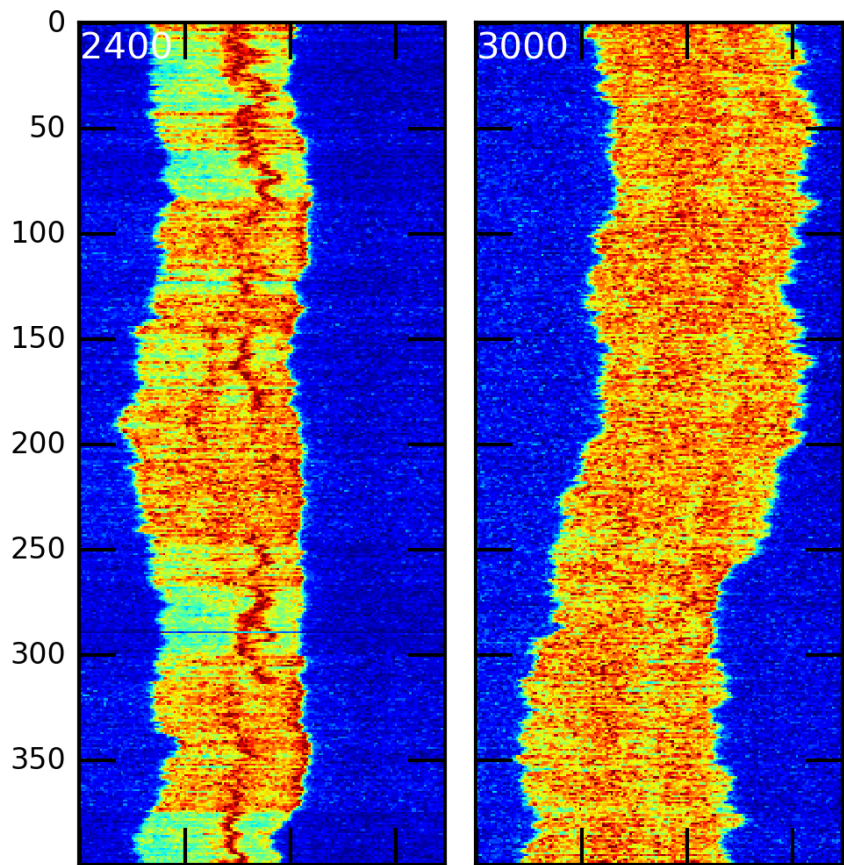


Figure 68: Vertical axis is time. White annotation gives channel width in nanometres.

4.41 130924-RecA-lambda-wide-4

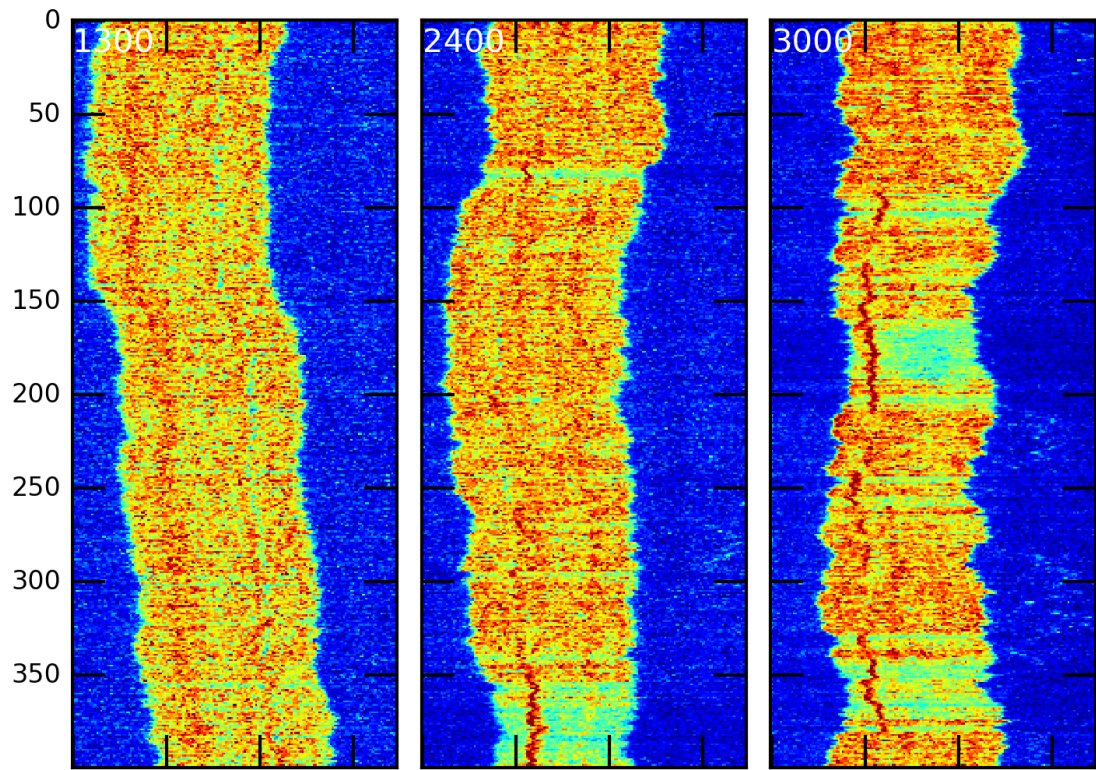


Figure 69: Vertical axis is time. White annotation gives channel width in nanometres.

4.42 130924-RecA-lambda-wide-5

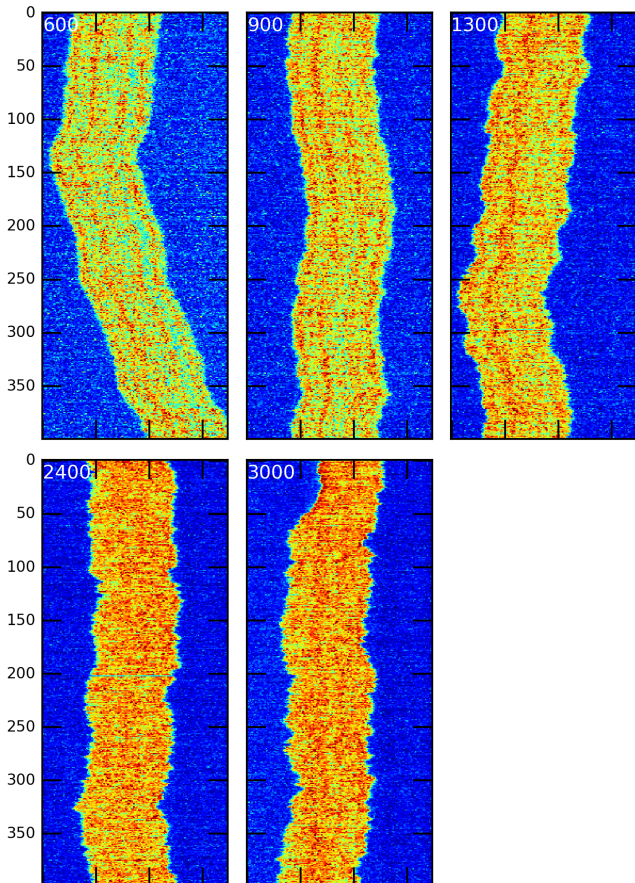


Figure 70: Vertical axis is time. White annotation gives channel width in nanometres.

4.43 130924-RecA-lambda-wide-8

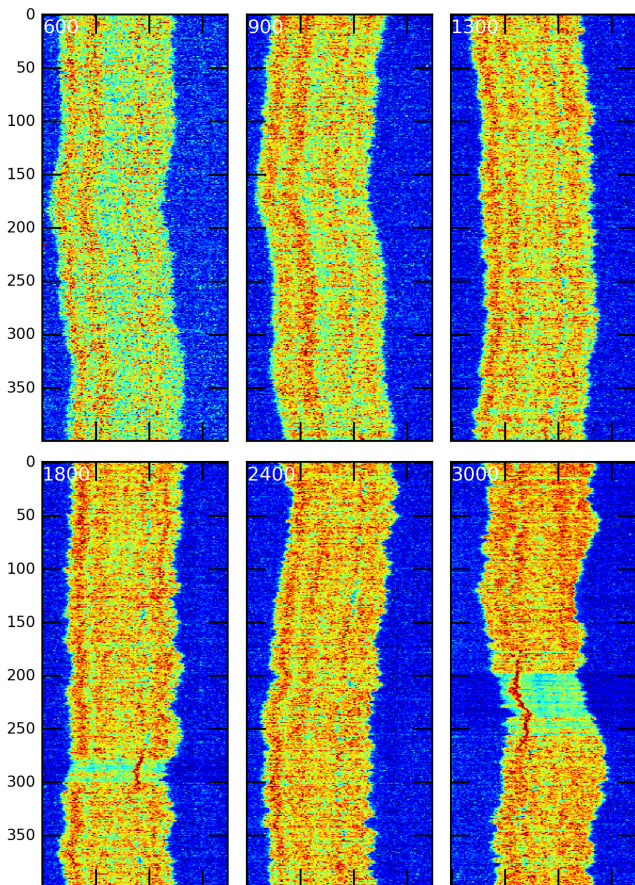


Figure 71: Vertical axis is time. White annotation gives channel width in nanometres.

4.44 130924-RecA-lambda-wide-9

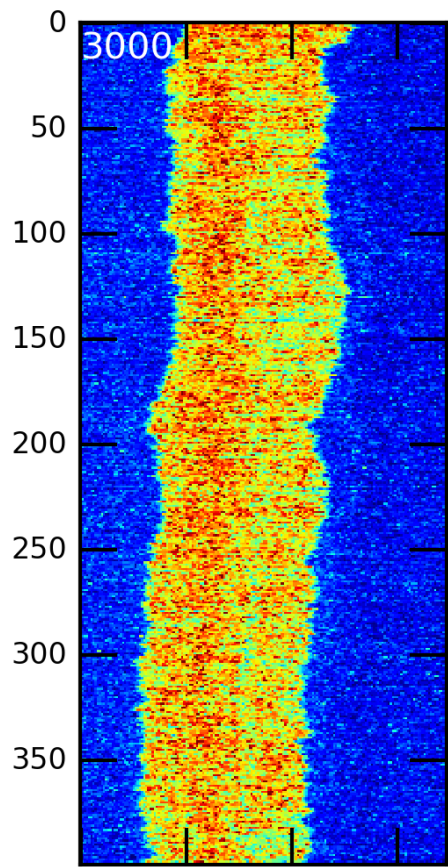


Figure 72: Vertical axis is time. White annotation gives channel width in nanometres.

References

- [1] K. Frykholm, M. Alizadehheidari, J. Fritzsche, J. Wigenius, M. Modesti, F. Persson, F. Westerlund, Probing physical properties of a dna-protein complex using nanofluidic channels, *Small* 10 (5) (2014) 884–887.
- [2] M. Hegner, S. B. Smith, C. Bustamante, Polymerization and mechanical properties of single reca-dna filaments, *Proceedings of the National Academy of Sciences* 96 (18) (1999) 10109–10114.